

## TYPE IA SUPERNOVAE STRONGLY INTERACTING WITH THEIR CIRCUMSTELLAR MEDIUM

JEFFREY M. SILVERMAN<sup>1,2,3</sup>, PETER E. NUGENT<sup>4</sup>, AVISHAY GAL-YAM<sup>5</sup>, MARK SULLIVAN<sup>6</sup>, D. ANDREW HOWELL<sup>7,8</sup>, ALEXEI V. FILIPPENKO<sup>2</sup>, IAIR ARCAVI<sup>5</sup>, SAGI BEN-AMI<sup>5</sup>, JOSHUA S. BLOOM<sup>2</sup>, S. BRADLEY CENKO<sup>2</sup>, YI CAO<sup>9</sup>, RYAN CHORNOCK<sup>10</sup>, KELSEY I. CLUBB<sup>2</sup>, ALISON L. COIL<sup>11</sup>, RYAN J. FOLEY<sup>9,12</sup>, MELISSA L. GRAHAM<sup>7,8</sup>, CHRISTOPHER V. GRIFFITH<sup>13</sup>, ASSAF HORESH<sup>9</sup>, MANSI M. KASLIWAL<sup>14</sup>, SHRINIVAS R. KULKARNI<sup>9</sup>, DOUGLAS C. LEONARD<sup>15</sup>, WEIDONG LI<sup>2,16</sup>, THOMAS MATHESON<sup>17</sup>, ADAM A. MILLER<sup>2</sup>, MARYAM MODJAZ<sup>18</sup>, ERAN O. OFEK<sup>5</sup>, YEN-CHEN PAN<sup>19</sup>, DANIEL A. PERLEY<sup>9</sup>, DOVI POZNANSKI<sup>20</sup>, ROBERT M. QUIMBY<sup>21</sup>, THEA N. STEELE<sup>2,22</sup>, ASSAF STERNBERG<sup>23</sup>, DONG XU<sup>5</sup>, AND OFER YARON<sup>5</sup>

*Draft version October 8, 2018*

### ABSTRACT

Owing to their utility for measurements of cosmic acceleration, Type Ia supernovae (SNe) are perhaps the best-studied class of SNe, yet the progenitor systems of these explosions largely remain a mystery. A rare subclass of SNe Ia show evidence of strong interaction with their circumstellar medium (CSM), and in particular, a hydrogen-rich CSM; we refer to them as SNe Ia-CSM. In the first systematic search for such systems, we have identified 16 SNe Ia-CSM, and here we present new spectra of 13 of them. Six SNe Ia-CSM have been well-studied previously, three were previously known but are analyzed in-depth for the first time here, and seven are new discoveries from the Palomar Transient Factory. The spectra of all SNe Ia-CSM are dominated by H $\alpha$  emission (with widths of  $\sim 2000$  km s<sup>-1</sup>) and exhibit large H $\alpha$ /H $\beta$  intensity ratios (perhaps due to collisional excitation of hydrogen via the SN ejecta overtaking slower-moving CSM shells); moreover, they have an almost complete lack of He I emission. They also show possible evidence of dust formation through a decrease in the red wing of H $\alpha$  75–100 d past maximum brightness, and nearly all SNe Ia-CSM exhibit strong Na I D absorption from the host galaxy. The absolute magnitudes (uncorrected for host-galaxy extinction) of SNe Ia-CSM are found to be  $-21.3 \leq M_R \leq -19$  mag, and they also seem to show ultraviolet emission at early times and strong infrared emission at late times (but no detected radio or X-ray emission). Finally, the host galaxies of SNe Ia-CSM are all late-type spirals similar to the Milky Way, or dwarf irregulars like the Large Magellanic Cloud, which implies that these objects come from a relatively young stellar population. This work represents the most detailed analysis of the SN Ia-CSM class to date.

*Subject headings:* supernovae: general — supernovae: individual (SN 1997cy, SN 1999E, SN 2002ic, SN 2005gj, SN 2008J, SN 2008cg, SN 2011jb, CSS120327:110520–015205, PTF11kx, PTF10htz, PTF10iuf, PTF10yni, PTF11dsb, PTF11hzx, PTF12efc, PTF12hnr) — stars: circumstellar matter

### 1. INTRODUCTION

While Type Ia supernovae (SNe Ia) have been used as precise distance indicators for nearly two decades (Phillips 1993), the nature of their progenitor systems and explosion mechanisms is still unclear (see Howell 2011, for further information). While there is general acceptance that they are the result of the thermonuclear explosion of C/O white dwarfs (WDs), it is now likely that there are at least two major channels that lead to a SN Ia. The single-degenerate (SD) channel occurs when the WD accretes matter from a nondegenerate companion star (e.g., Whelan & Iben 1973), while the double-degenerate (DD) channel is the result of the merger of two WDs (e.g., Iben & Tutukov 1984; Webbink 1984).

Extremely nearby SNe Ia which were discovered soon after explosion have recently led to tight constraints on

Physics, Department of Physics, New York, NY 10003, USA.

<sup>19</sup> Department of Physics (Astrophysics), University of Oxford, Keble Road, Oxford OX1 3RH, UK.

<sup>20</sup> School of Physics and Astronomy, Tel Aviv University, Tel Aviv, Israel.

<sup>21</sup> Kavli IPMU, The University of Tokyo, Kashiwanoha 5-1-5, Kashiwa, 277-8583, Japan.

<sup>22</sup> Department of Computer Science, Kutztown University of Pennsylvania, Kutztown, Pennsylvania 19530, USA.

<sup>23</sup> Max-Planck-Institut für Astrophysik, 85741 Garching, Germany.

<sup>1</sup> Department of Astronomy, University of Texas, Austin, TX 78712-0259, USA.

<sup>2</sup> Department of Astronomy, University of California, Berkeley, CA 94720-3411, USA.

<sup>3</sup> email: jsilverman@astro.as.utexas.edu.

<sup>4</sup> Lawrence Berkeley National Laboratory, Berkeley, CA 94720, USA.

<sup>5</sup> Benoziyo Center for Astrophysics, The Weizmann Institute of Science, Rehovot 76100, Israel.

<sup>6</sup> School of Physics and Astronomy, University of Southampton, Southampton, SO17 1BJ, UK.

<sup>7</sup> Las Cumbres Observatory Global Telescope Network, Goleta, CA 93117, USA.

<sup>8</sup> Department of Physics, University of California, Santa Barbara, CA 93106, USA.

<sup>9</sup> Cahill Center for Astrophysics, California Institute of Technology, Pasadena, CA 91125, USA.

<sup>10</sup> Harvard-Smithsonian Center for Astrophysics, Cambridge, MA 02138, USA.

<sup>11</sup> Department of Physics, University of California, San Diego, La Jolla, CA 92093, USA.

<sup>12</sup> Clay Fellow.

<sup>13</sup> Department of Astronomy and Astrophysics, The Pennsylvania State University, University Park, PA 16802, USA.

<sup>14</sup> Observatories of the Carnegie Institution of Science, Pasadena, CA 91101, USA.

<sup>15</sup> Department of Astronomy, San Diego State University, San Diego, CA 92182-1221, USA.

<sup>16</sup> Deceased 12 December 2011.

<sup>17</sup> National Optical Astronomy Observatory, Tucson, AZ 85719-4933, USA.

<sup>18</sup> New York University, Center for Cosmology and Particle

the size and luminosity of the companion star, thus ruling out many plausible SD scenarios for these objects (e.g., Nugent et al. 2011; Ganeshalingam et al. 2011; Brown et al. 2012; Foley et al. 2012b; Bloom et al. 2012; Silverman et al. 2012b). In addition, the so-called super-Chandrasekhar mass SNe Ia are thought to contain  $> 1.4 M_{\odot}$  of SN ejecta and thus are likely formed from the DD scenario (e.g., Howell et al. 2006; Yamanaka et al. 2009; Scalzo et al. 2010; Silverman et al. 2011; Taubenberger et al. 2011). However, there are a few SNe Ia that show strong evidence for the SD channel, possibly with a red giant (RG) companion. Photoionization and subsequent recombination of circumstellar medium (CSM) has been observed in relatively normal SNe Ia (Patat et al. 2007; Blondin et al. 2009; Simon et al. 2009), and CSM has been detected in the spectra of at least 20% of SNe Ia in spiral galaxies (Sternberg et al. 2011) and has been linked to SN Ia explosion properties (Foley et al. 2012a).

Even greater interaction with CSM has been seen in a small number of SNe Ia whose spectra contain strong, narrow hydrogen emission and whose luminosities often exceed those of the more “typical” SNe Ia that follow the light-curve decline rate versus peak luminosity correlation (i.e., the “Phillips relation”; Phillips 1993). These “hybrid” objects resemble Type II<sub>n</sub> SNe (SNe II<sub>n</sub>) and have been dubbed SNe Ia/II<sub>n</sub>, Ian, IIa, and IIan. Under the standard SN classification scheme (e.g., Filippenko 1997), any SN with hydrogen features in its optical spectrum is considered a Type II SN and the subset of these showing relatively narrow emission lines are referred to as SNe II<sub>n</sub>. Objects with relatively narrow hydrogen emission lines that are further linked (spectroscopically) to SNe Ia could be denoted as “Type II<sub>n</sub>a,” though this moniker is somewhat cumbersome and obfuscating. Therefore, in this work, we choose to label such events as “SNe Ia-CSM” (or sometimes as “Ia-CSM objects”) to highlight the connection to the physically distinct Type Ia class.

SNe Ia-CSM have spectra which appear to be “diluted” SN Ia spectra with the aforementioned narrow hydrogen emission lines superposed (leading to the SN II<sub>n</sub> resemblance). Their light curves are broad and quite long-lived, peaking at absolute magnitudes brighter than about  $-19$  mag. The two best-studied objects in this class are SNe 2002ic and 2005gj (Hamuy et al. 2003; Deng et al. 2004; Kotak et al. 2004; Wang et al. 2004; Wood-Vasey et al. 2004; Aldering et al. 2006; Prieto et al. 2007). Until recently there was some debate in the literature as to whether these objects are truly SNe Ia or are in fact some strange flavor of core-collapse SN (CCSN; e.g., Benetti et al. 2006; Trundle et al. 2008).

This possible controversy seems to have been settled by the discovery and analysis of PTF11kx (Dilday et al. 2012; Silverman et al. submitted). This object was discovered by the Palomar Transient Factory (PTF; Rau et al. 2009; Law et al. 2009) and shown to initially resemble the somewhat overluminous Type Ia SN 1999aa (Li et al. 2001; Strolger et al. 2002; Garavini et al. 2004). Optical spectra of PTF11kx soon developed a strong  $H\alpha$  feature with a P-Cygni profile, eventually resembling spectra of SNe 2002ic and 2005gj, the previously mentioned best-studied SNe Ia-CSM. Using early-time data, Dilday et al. (2012) find that PTF11kx was a *bona fide* SN Ia

with a symbiotic nova progenitor (i.e., a SD scenario). Analyzing late-time data, (Silverman et al. submitted) present further evidence that PTF11kx was a SN Ia that is strongly interacting with multiple thin CSM shells. These findings can logically be extended to imply that *all* SNe Ia-CSM are likely to be real SNe Ia with significant amounts of H-rich CSM, possibly caused in part by a nondegenerate companion.

In §2 we discuss our search for and identification (or reidentification) of previously known SNe Ia-CSM. Most of these have not been studied in much detail before, and we present new spectra of many of them. Similarly, in §3, we discuss new SNe Ia-CSM discovered by PTF. §4 contains the analysis of our spectra of all SNe Ia-CSM presented herein, in addition to the spectra of PTF11kx from Dilday et al. (2012) and Silverman et al. (submitted). Finally, we recap our conclusions in §5 and summarize the major observational characteristics shared by all SNe Ia-CSM.

## 2. PREVIOUSLY KNOWN SNE IA-CSM

In order to find SNe Ia-CSM that may have previously been classified as SNe II<sub>n</sub>, we use the SuperNova IDentification code (SNID; Blondin & Tonry 2007). SNID classifies SN spectra by cross-correlating an input spectrum with a large database of observed SN spectra (known as “templates”). To identify SNe Ia-CSM, we created a special set of spectral templates that consisted of all 310 spectra of 163 objects classified as SNe II<sub>n</sub> from the Berkeley SN Group’s database (Silverman et al. 2012a). In addition to these, we also included templates of a handful of underluminous, overluminous, and normal SNe Ia at a variety of epochs, as well as 27 spectral templates of the well-known Ia-CSM objects SNe 2002ic and 2005gj (mentioned in §1).

We then ran all of our spectra of PTF11kx and the previously known Ia-CSM objects SNe 1999E, 2002ic, and 2005gj (see §§2.1, 2.2) through SNID using this newly created template set, making sure to ignore any templates made from the object currently under consideration. The best-matching templates for each of these known SNe Ia-CSM were visually inspected, and SNe which were often found in the top 10–20 best-matching templates were flagged for further examination. This yielded 18 possible SNe Ia-CSM. Upon deeper analysis, it was found that many of the spectra matched those of SNe Ia-CSM and “normal” SNe II<sub>n</sub> equally well; also, spectra of some objects had very low signal-to-noise ratios. While some of these may perhaps be true SNe Ia-CSM, we cannot confidently claim this for most of them. Thus, after this closer inspection was conducted, four of the 18 possible SNe Ia-CSM are convincingly part of the SN Ia-CSM class.

Interestingly, all four of our “newly discovered” members of the SN Ia-CSM class were noted to be similar to the prototypical Ia-CSM objects SNe 2002ic and 2005gj, but only in unrefereed spectral classifications. From a literature search, no mention of these objects as SNe Ia-CSM is found anywhere else, except for SN 2008J which was studied by Taddia et al. (2012), work that was made public during the final stages of preparing this manuscript. Adding these four objects to the prototypical SNe 2002ic and 2005gj and to the less-studied, but still fairly well known Ia-CSM objects SNe 1997cy and

1999E gives us a sample size of eight SNe Ia-CSM out of the hundreds of SNe IIn discovered in the last  $\sim 15$  yr. Tables 1 and 2 give basic information for all eight of these SNe Ia-CSM and their host galaxies, respectively, and our spectra of six of these SNe are summarized in Table 3. Upon publication, all spectra presented in this paper will be available in electronic format on WISeREP (the Weizmann Interactive Supernova data REPOSITORY; Yaron & Gal-Yam 2012).<sup>24</sup> These eight SNe Ia-CSM are briefly discussed (in pairs) below.

### 2.1. SN 2002ic and SN 2005gj

As already mentioned, the two prototypical and best-studied SNe Ia-CSM are SN 2002ic (Hamuy et al. 2003; Deng et al. 2004; Kotak et al. 2004; Wang et al. 2004; Wood-Vasey et al. 2004) and SN 2005gj (Aldering et al. 2006; Prieto et al. 2007). The photometric and spectral evolution of these two objects has been well-studied in the works cited above. Both were found to be more luminous than typical SNe Ia and most SNe IIn, have spectra consisting of relatively narrow  $H\alpha$  emission (with P-Cygni profiles) on top of a “diluted” SN Ia spectrum, and broad, slowly evolving light curves. To the already impressive data on SN 2005gj in the literature, we add five spectra (three at early times and two at very late times) that were originally published by Silverman et al. (2012a) and are displayed in Figure 1.

### 2.2. SN 1997cy and SN 1999E

The two next-best-studied SNe Ia-CSM are SN 1997cy (Turatto et al. 2000; Germany et al. 2000) and SN 1999E (Filippenko 2000; Rigon et al. 2003). Neither of these objects have as much data as either SNe 2002ic or 2005gj, but they have still been studied fairly rigorously due to their peculiar nature (especially before the discovery of SNe 2002ic and 2005gj). Again, both objects showed relatively bright absolute magnitudes with spectra that somewhat resembled those of SNe Ia with superposed  $H\alpha$  emission. In Figure 2 we plot our six spectra of SN 1999E, which were first published by Filippenko (2000), before it was realized that this was a SN Ia. Unfortunately, it seems that SN 1999E was discovered well after maximum brightness; thus, the phases displayed in Figure 2 are relative to the UT date of discovery (1999 Jan. 15; Rigon et al. 2003), and are likely from a much later phase if calculated relative to maximum brightness.

### 2.3. SN 2008J and SN 2008cg

SNe 2008J and 2008cg were both claimed to resemble SNe 2002ic and 2005gj in unrefereed classification circulars (Stritzinger et al. 2008; Filippenko et al. 2008), and very recently Taddia et al. (2012) has published an analysis of SN 2008J. Fox et al. (2011) investigated the  $H\alpha$  profiles and presented mid-infrared (IR) photometry from a *Spitzer*/IRAC survey of these objects (referred to as simply “SNe IIn”) and found that both SNe were clearly detected in the mid-IR  $\sim 500$ –600 d after discovery (see §4.3 for more information). SN 2008J resembles SN 2005gj in an optical spectrum obtained only 2 d after discovery (Stritzinger et al. 2008), which is  $\sim 2.5$  weeks

before  $r$ -band maximum brightness (Taddia et al. 2012), and it continues to resemble SNe Ia-CSM in all nine of our spectra (plotted in Figure 3). Taddia et al. (2012) also found that the optical and NIR spectra of SN 2008J show narrow H Balmer, Paschen, and Brackett emission (most with P-Cygni profiles) and that the optical spectra could be decomposed into a low-order polynomial continuum and the spectrum of the overluminous Type Ia SN 1991T. On the other hand, an optical spectrum of SN 2008cg resembles a relatively normal SN IIn 3 d after discovery (Blondin & Calkins 2008), which is about 10 d past maximum brightness. However, by  $\sim 2$  m past discovery, SN 2008cg was found to closely resemble SNe 2002ic and 2005gj (Filippenko et al. 2008). Our five spectra of this objects are shown in Figure 4. Note that the data on SNe 2008J and 2008cg presented here are the same optical spectra discussed by Fox et al. (2011).

### 2.4. SN 2011jb and CSS120327:110520–015205

Almost nothing has appeared in the literature regarding SNe 2011jb and CSS120327:110520–015205 (Drake et al. 2012), despite both objects being immediately classified as SNe Ia-CSM (Kankare et al. 2011; Drake et al. 2012). We present our three spectra of SN 2011jb and our two spectra of CSS120327:110520–015205 in Figure 5.

## 3. PTF IA-CSM OBJECTS

A similar search for SNe Ia-CSM was performed using 178 spectra of all 63 SNe IIn discovered by PTF through August 2012. Once again, we ran these spectra through SNID to see if they were well matched to our sample of SNe Ia-CSM. This initial analysis yielded nine possible objects, but two of these were rejected based on equally good spectral matches to SNe IIn. We classify the seven remaining objects as true SNe Ia-CSM. These PTF objects (in addition to PTF11kx) and their host galaxies are summarized in Tables 4 and 5, and our spectra of them are described in Table 6 and displayed in Figures 6–11. See Dilday et al. (2012) and Silverman et al. (submitted) for further information regarding PTF11kx and its spectra.

Three of the PTF SNe Ia-CSM were publicly announced while the other four were not. PTF10htz was initially classified as a Type IIb SN (Arcavi et al. 2010b), but our careful SNID analysis shows that it is likely a SN Ia-CSM (with substantial host-galaxy contamination) and matches SNe 2011jb and 2005gj (Fig. 6). In Arcavi et al. (2010a), PTF10yni (which was independently discovered by Drake et al. 2010, and called CSS101008:001049+141039) was classified as a “IIn/Ic,” but once again our SNID analysis indicates that it is actually a SN Ia-CSM, matching SN 2005gj (Fig. 8). Finally, PTF11dsb was classified simply as a “SN II” by Gal-Yam et al. (2011), but our analysis here shows that it is possibly a SN Ia-CSM, somewhat similar to SN 2011jb (Fig. 8), though it is not completely clear whether this object is a *bona fide* member of the class.

## 4. ANALYSIS AND DISCUSSION OF THE SN IA-CSM CLASS

Using our SNID analysis we have identified seven new SNe Ia-CSM from PTF (§3) and reidentified eight previously known SNe Ia-CSM (§2). Given these 15 objects, in addition to PTF11kx, we now attempt to define observational characteristics of this class of SNe Ia (while keep-

<sup>24</sup> <http://www.weizmann.ac.il/astrophysics/wiserep> .

TABLE 1  
NON-PTF SNE Ia-CSM

SN Name	Discovery Date	Approx. Date of Maximum	Discovery Reference	Classification Reference <sup>a</sup>	Peak Absolute Magnitude <sup>b</sup>	Galactic Reddening <sup>c</sup>
SN 1997cy	1997 July 16	... <sup>d</sup>	IAUC 6706	T00, G00	$< -20.1$ ( <i>V</i> )	0.021
SN 1999E	1999 Jan. 15	... <sup>d</sup>	IAUC 7089	IAUC 7090, R03	$< -19.5$ ( <i>V</i> )	0.088
SN 2002ic	2002 Nov. 13	2002 Nov. 27	IAUC 8019	IAUC 8028	$< -20.3$ ( <i>V</i> )	0.059
SN 2005gj	2005 Sep. 26	2005 Oct. 14	CBET 247	CBET 302	$-20.2$ ( <i>g</i> )	0.121
SN 2008J	2008 Jan. 15	2008 Feb. 3	CBET 1211	CBET 1218	$-19.2$ ( <i>r</i> )	0.023
SN 2008cg	2008 May 5	2008 Apr. 29	CBET 1366	CBET 1420	$-19.4$ (unf)	0.050
SN 2011jb	2011 Nov. 28	... <sup>d</sup>	CBET 2947	CBET 2947	$-20.3$ ( <i>R</i> )	0.034
CSS120327:110520-015205	2012 Mar. 27	2012 Mar. 8	ATel 4081	ATel 4081	$-20.5$ (unf)	0.052

<sup>a</sup> ‘T00’ = Turatto et al. (2000); ‘G00’ = Germany et al. (2000); ‘R03’ = Rigon et al. (2003).  
<sup>b</sup> The optical band of the peak absolute magnitude (and approximate date of maximum brightness) is given in parentheses; ‘unf’ = unfiltered.  
<sup>c</sup> Galactic reddening toward each SN as derived from the dust maps of Schlegel et al. (1998); includes the corrections of Peek & Graves (2010).  
<sup>d</sup> SN was discovered after maximum brightness.

TABLE 2  
NON-PTF Ia-CSM HOST GALAXIES

SN Name	Name	Type	Redshift <i>z</i>
SN 1997cy	Sersic 040/06:[GGP90] 342	Dwarf Irregular	0.0642
SN 1999E	GSC 6116 00964	Late-Type Spiral	0.0258
SN 2002ic	NEAT J013002.81+215306.9	Late-Type Spiral (Sbc)	0.0660
SN 2005gj	SDSS J030111.99-003313.9	Dwarf Irregular	0.0616
SN 2008J	MCG -02-07-033	Late-Type Spiral (SBbc)	0.0159
SN 2008cg	FGC 1965	Late-Type Spiral (Scd)	0.0362
SN 2011jb	SDSS J113704.81+152813.9	Dwarf Irregular	0.0826
CSS120327:110520-015205	SDSS J110520.10-015204.9	Dwarf Irregular	0.0908

ing in mind that PTF11kx may be an extreme member). Though no single observable appears to be a sufficient condition for a SN to be considered a Ia-CSM object, there seem to be a handful of features that nearly all of the SNe Ia-CSM display. These are discussed in detail below, along with a few observables that are also found more generally in “normal” SNe IIn.

#### 4.1. Optical Photometry of SNe Ia-CSM

The Caltech Core-Collapse Project (CCCP; Kiewe et al. 2012) found that the typical peak absolute magnitude range for SNe IIn is  $-18.7 \leq M_R \leq -17$  mag (using  $H_0 = 73 \text{ km s}^{-1} \text{ Mpc}^{-1}$ , the value adopted throughout this work), while the Lick Observatory SN Search (LOSS) found their SNe IIn to have peak luminosities in the range  $-19 \leq M_R \leq -16$  mag (Li et al. 2011). LOSS also showed that SNe IIP/IIL have an overlapping range of peak absolute magnitudes ( $-17 \leq M_R \leq -15$  mag; Smith et al. 2011a), but the spectra of SNe IIP/IIL differ significantly from those of SNe IIn or SNe Ia-CSM (the former consisting of broad P-Cygni profiles of H Balmer lines; e.g., Filippenko 1997). On the less luminous end, luminous blue variable star (LBV) outbursts and so-called “SN impostors” (which are spectroscopically similar to SNe IIn and SNe Ia-CSM) have peak absolute magnitudes  $-16 \leq M_R$  mag (Smith et al. 2011a). On the more luminous end, Type II superluminous SNe (which can also resemble SNe IIn and SNe Ia-CSM spectroscopically) have peak luminosities  $M_R \lesssim -21$  mag (Gal-Yam 2012; Quimby et al. 2013). We note that both CCCP and LOSS have a dearth of objects which are spectroscopically similar to SNe IIn with peak absolute mag-

nitudes  $-21 \leq M_R \leq -19$  mag, although the PTF sample contains quite a few objects in this range (Fig. 12).

Extending this analysis, in Figure 12 we plot the peak absolute *r*-band magnitude of all 63 objects spectroscopically identified as SNe IIn by PTF through August 2012. The photometric calibration of the PTF data is based on the Sloan Digital Sky Survey (SDSS) data when possible, otherwise the PTF calibration and natural magnitude system are used (Ofek et al. 2012a,b). The vertical dotted lines denote the boundaries between the various subtypes of SNe IIn (LBV outbursts and SN impostors, typical SNe IIn, and superluminous SNe II) and our proposed range of SN Ia-CSM luminosities. The gray shaded region is the range of SNe Ia that follow the Phillips relation, about  $-19.7$  to  $-18.5$  mag (e.g., Ganeshalingam et al. 2010). The black, filled histogram shows the peak absolute magnitudes of the seven SNe Ia-CSM discovered by PTF (§3) not including PTF11kx, the downward-pointing arrows signify the peak luminosities of the eight previously known SNe Ia-CSM (§2), and the star represents the peak absolute magnitude of PTF11kx (Dilday et al. 2012).

TABLE 3  
SPECTRA OF NON-PTF SNE IA-CSM

UT Date	Age (d) <sup>a</sup>	Instrument <sup>b</sup>	Range (Å)	Res. (Å) <sup>c</sup>	Exp. (s)
SN 1999E <sup>d</sup>					
1999 Jan. 19.7	4	LRIS	5120–8850	7	200
1999 Jan. 20.7	5	LRIS	3760–6240	4.5	200
1999 Jan. 21.7	6	LRIS	6450–10200	7	300
1999 Feb. 12.5	27	Kast	3382–10500	6/11	1800
1999 Feb. 23.5	38	Kast	3366–10550	6/11	1200
1999 Mar. 12.5	55	Kast	3442–10466	6/11	1800
SN 2005gj <sup>e</sup>					
2005 Dec. 2.4	46	DEIMOS	3897–9070	3	300
2005 Dec. 4.4	48	LRIS	3280–9320	4.5/7	300
2006 Jan. 1.4	74	DEIMOS	3918–9061	3	600
2006 Dec. 23.4	409	DEIMOS	4496–9574	3	1500
2007 Feb. 14.3	459	LRIS	3206–9238	6.4/7	1200
SN 2008J					
2008 Feb. 16.2	12	Kast	4440–10500	4.9/11.9	900
2008 Aug. 1.5	177	Kast	4292–10800	6.0/11.0	900
2008 Aug. 26.5	201	Kast	4232–10800	6.7/12.3	900
2008 Sep. 7.5	213	Kast	4050–10740	7.4/12.3	1200
2008 Sep. 22.5	228	Kast	3488–10344	4.6/11.0	1200
2008 Oct. 7.5	243	Kast	3554–10780	4.4/11.0	1200
2008 Oct. 22.4	258	Kast	3476–6400	9.0	2400
2008 Nov. 20.3	286	Kast	3480–10000	5.0/11.0	1800
2008 Nov. 23.4	289	Kast	3420–8000	4.8/5.0	1200
SN 2008cg					
2008 May 8.4	9	Kast	3300–10800	5.4/11.6	1800
2008 May 15.4	15	Kast	3300–10800	5.5/11.7	1800
2008 June 29.3	59	Kast	3300–10790	5.9/10.8	1500
2008 July 7.3	67	Kast	3306–10800	6.0/11.3	1500
2008 Aug. 27.3	116	LRIS	3268–9240	4.5/7.0	454
SN 2011jb					
2011 Dec. 24.4	24	Kast	3518–10138	4.7/9.8	2400
2012 June 16.4	186	LRIS	3350–10152	3.6/6.1	600
2012 July 16.3	213	LRIS	3727–9939	3.7/6.4	600
CSS120327:110520–015205					
2012 May 17.2	64	LRIS	3343–10100	3.7/6.2	300
2012 June 16.3	92	LRIS	3346–10069	4.1/6.1	1200

<sup>a</sup>Rest-frame days relative to maximum brightness, except for SNe 1999E and 2011jb where the epoch is relative to the UT date of discovery (1999 Jan. 15 and 2011 Nov. 28, respectively). See Table 1 for the dates of maximum brightness for the rest of the objects.

<sup>b</sup>LRIS = Low Resolution Imaging Spectrometer on the Keck 10 m telescope; Kast = Kast double spectrograph on the Shane 3 m telescope at Lick Observatory; DEIMOS = DEep Imaging Multi-Object Spectrograph on the Keck 10 m telescope.

<sup>c</sup>Approximate full width at half-maximum intensity (FWHM) resolution. If two numbers are listed, they represent the blue-side and red-side resolutions, respectively.

<sup>d</sup>These spectra of SN 1999E have been previously published by Filippenko (2000).

<sup>e</sup>These spectra of SN 2005gj have been previously published by Silverman et al. (2012a).

TABLE 4  
PTF SNE IA-CSM

SN Name	Discovery Date	Approx. Date of <i>r</i> -Band Maximum	Peak Absolute <i>r</i> -Band Magnitude	Galactic Reddening <sup>a</sup>
PTF11kx	2011 Jan. 16	2011 Jan. 29	−19.3	0.053
PTF10htz	2010 Apr. 3	2010 May 16	−19.1	0.049
PTF10iuf	2010 June 5	2010 July 4	−20.5	0.021
PTF10yni	2010 Oct. 3	2010 Oct. 30	−20.6	0.059
PTF11dsb	2011 May 13	... <sup>b</sup>	−19.8	0.020
PTF11hzx	2011 July 17	2011 July 23	−21.3	0.096
PTF12efc	2012 May 13	2012 June 15	−21.0	0.015
PTF12hnr	2012 Aug. 7	... <sup>b</sup>	−21.0	0.037

<sup>a</sup>Galactic reddening toward each SN as derived from the dust maps of Schlegel et al. (1998); includes the corrections of Peek & Graves (2010).

<sup>b</sup>SN was discovered after maximum brightness.

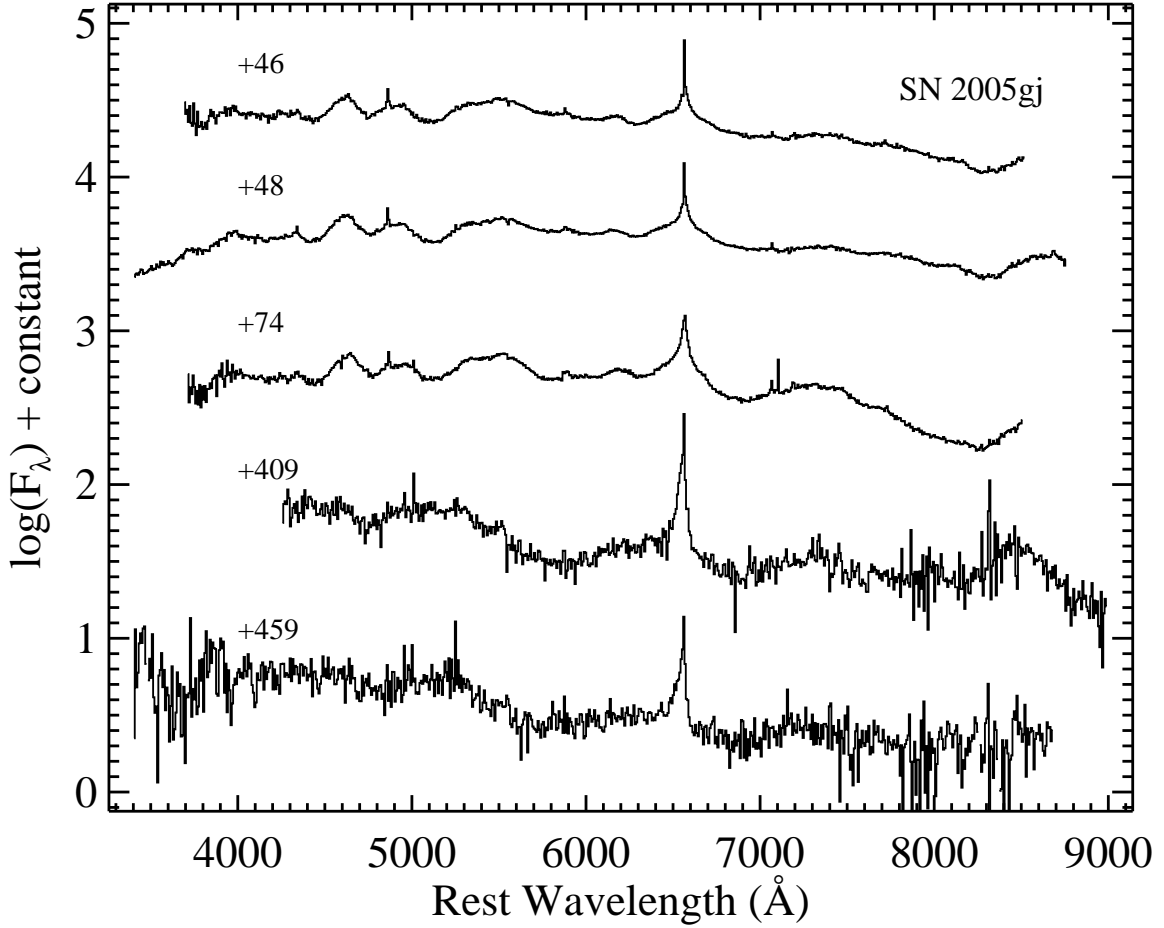


FIG. 1.— Spectra of SN 2005gj, originally published by Silverman et al. (2012a), labeled with age relative to maximum brightness. The data have had their host-galaxy recession velocity removed and have been corrected for Galactic reddening.

TABLE 5  
PTF IA-CSM HOST GALAXIES

SN Name	Name	Type	Redshift $z$
PTF11kx	SDSS J080913.20+461842.9	Late-Type Spiral	0.0466
PTF10htz	CGCG 352-058	Late-Type Spiral	0.0352
PTF10iuf	SDSS J160615.65+335213.2	Late-Type Spiral	0.1586
PTF10yni	...	...	0.1688
PTF11dsb	SDSS J161835.63+324150.0	Late-Type Spiral	0.1900
PTF11hzz	...	...	0.2287
PTF12efc	...	...	0.2341
PTF12hnr	SDSS J232415.43-051239.0	Late-Type Spiral	0.1883

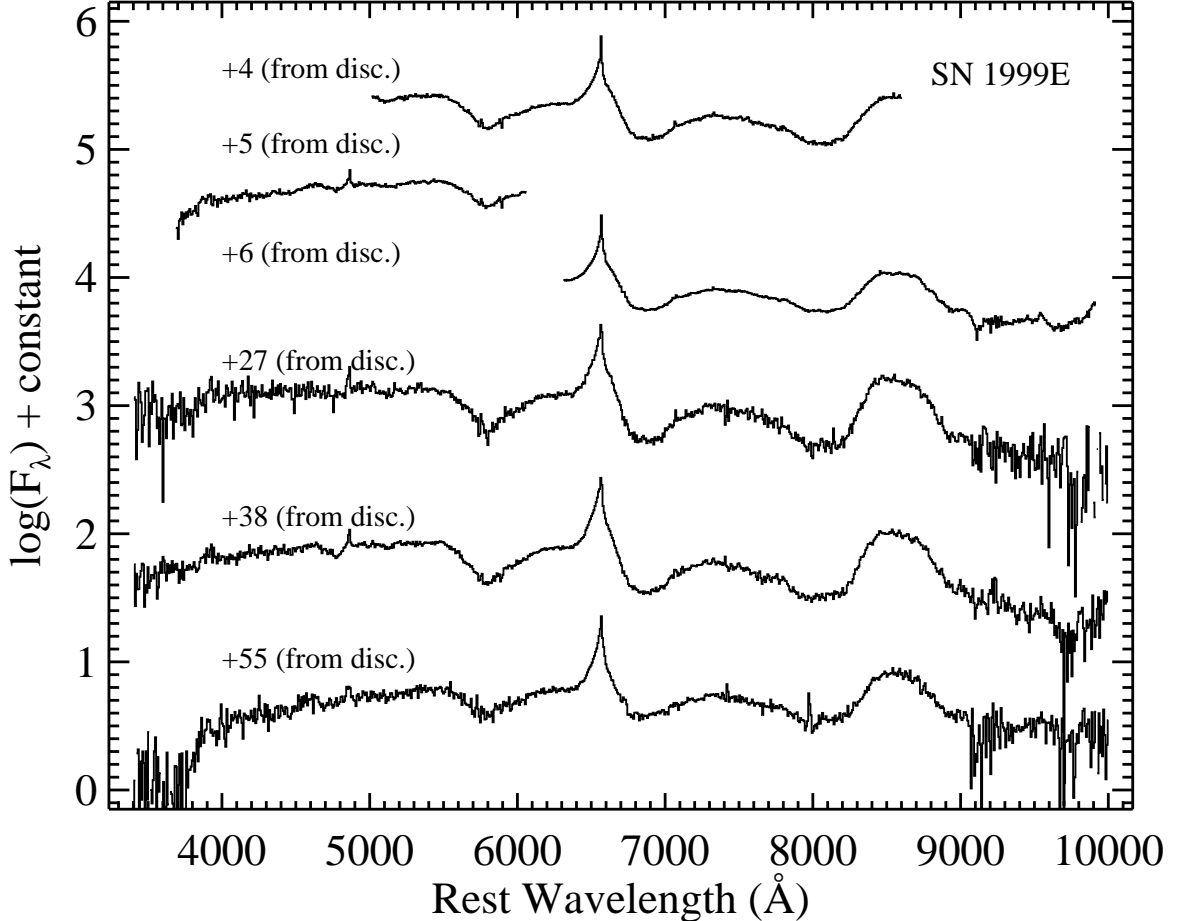


FIG. 2.— Spectra of SN 1999E, originally published in Filippenko (2000), labeled with age relative to the discovery date. The data have had their host-galaxy recession velocity removed and have been corrected for Galactic reddening.

As seen in Figure 12, 15 of the 16 SNe Ia-CSM discussed in this paper fall in the luminosity range  $-21 \leq M_R \leq -19$  mag. The one outlier, PTF11hxx, just barely misses this cutoff with peak luminosity  $M_R = -21.3$  mag. It appears that SNe Ia-CSM *must* have an absolute optical magnitude in this range, roughly 0.5–1.5 mag brighter than their more normal SN Ia cousins, likely due to the interaction of the SN ejecta with the CSM (which gives SNe Ia-CSM their distinct spectra).

We also investigate the rise times of SN Ia-CSM light curves (i.e., the time elapsed between explosion and maximum brightness). Ganeshalingam et al. (2011) found that normal SNe Ia have a rise time of  $\sim 18$  d in the  $B$  band and  $\sim 20$  d in the  $V$  band (after correcting for light-curve shape). Longer rise times have been seen in more exotic SN Ia subtypes, with possible super-Chandrasekhar mass SNe Ia having rise times of  $\sim 24$  d (e.g., Scalzo et al. 2010; Silverman et al. 2011).

Accurate rise-time measurements require photometric observations well before maximum brightness; thus, not many of the previously studied SNe Ia-CSM have reasonable rise-time constraints. SN 2002ic was found to have a rise time as long as 28 d (Wood-Vasey et al. 2004), while SN 2005gj had a rise time of  $\sim 20$  d in the  $g$  band and possibly up to  $\sim 32$  d in the  $r$  band (Aldering et al. 2006; Prieto et al. 2007). On the other hand, CSS120327:110520–

015205 appeared to have a rise time of  $\sim 45$  d (Drake et al. 2012). As for the PTF SNe Ia-CSM, Dilday et al. (2012) used a rise time of  $\sim 20$  d for PTF11kx. Five of the seven other SNe Ia-CSM from PTF have constraining pre-maximum brightness photometry and show evidence for relatively long rise times ( $\sim 30$ – $40$  d).

Thus, it appears that SNe Ia-CSM tend to have longer rise times than more normal SNe Ia. This is consistent with the idea that the rise time is related to the photon diffusion time (which should be longer in SNe Ia-CSM as the light must make its way out of the relatively large amount of CSM) as well as models of circumstellar shells in symbiotic recurrent nova systems (Moore & Bildsten 2012). These rise times can also be used to estimate the mass-loss rate of the progenitor system that gave rise to the CSM. Using typical SN Ia-CSM ejecta and wind velocities of a few thousand and  $100 \text{ km s}^{-1}$ , respectively, and equations in Ofek et al. (2013), we find that SNe Ia-CSM have mass-loss rates of a few times  $10^{-1} M_{\odot} \text{ yr}^{-1}$ .

#### 4.2. Optical Spectroscopy of SNe Ia-CSM

We identified SNe Ia-CSM using our SNID analysis outlined in §2 and §3. These matches were based solely on comparing low-resolution optical spectra of input SNe with a library of template spectra. When comparing the spectra of the SNe Ia-CSM, some show relatively

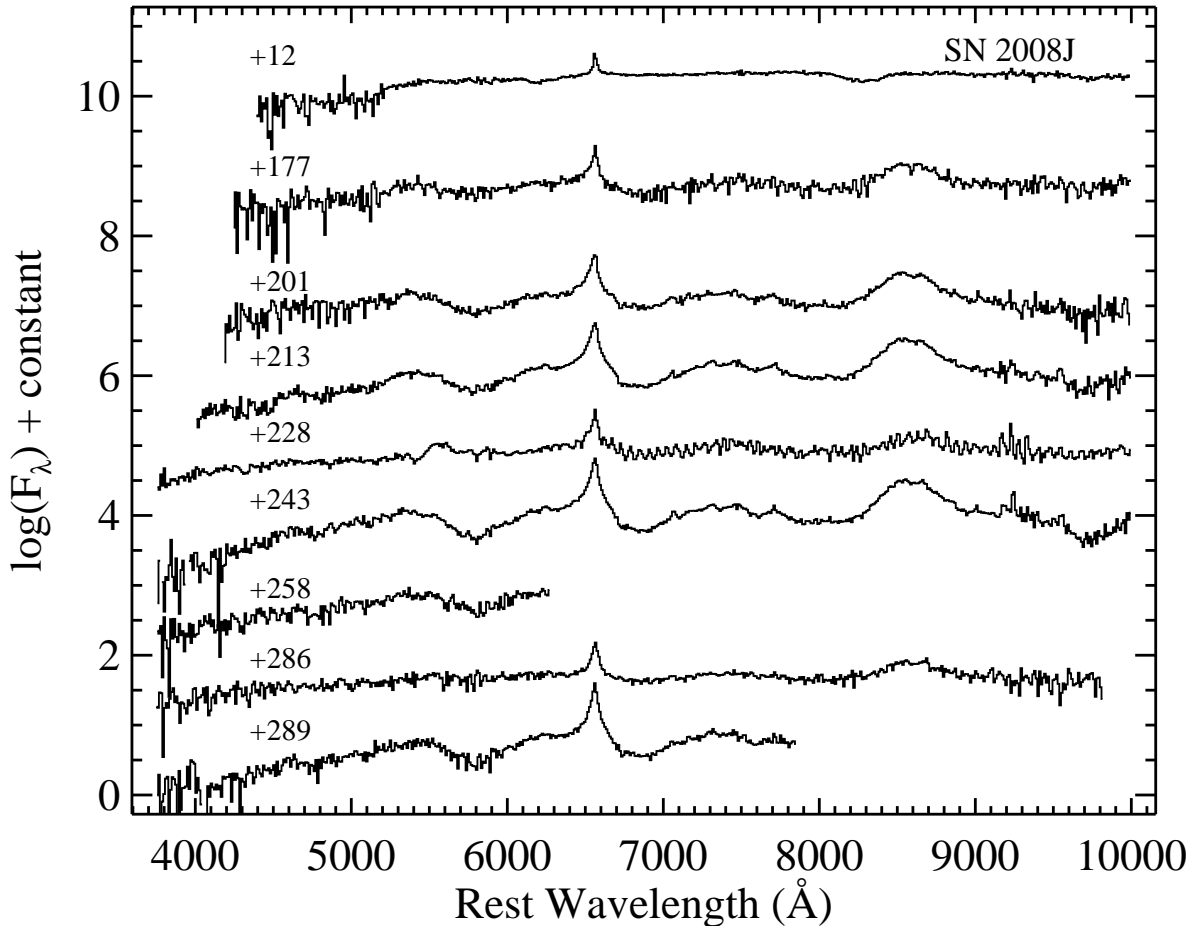


FIG. 3.— Spectra of SN 2008J, the  $H\alpha$  profiles of which were analyzed by Fox et al. (2011), labeled with age relative to maximum brightness. The data have had their host-galaxy recession velocity removed and have been corrected for Galactic reddening.

strong underlying SN Ia features (e.g., SNe 2002ic and 2005gj, and especially PTF11kx), mostly at early times and often resembling the somewhat overluminous Type Ia SN 1999aa (Li et al. 2001; Strolger et al. 2002; Garavini et al. 2004). However, other SNe Ia-CSM (mostly ones with spectra from later epochs) do not resemble any subtype of SN Ia, aside from the other SNe Ia-CSM, and are much more easily mistaken for more typical SNe IIn.

At these late times, the spectra of SNe Ia-CSM basically consist of a relatively blue “quasi-continuum,” which is likely due to emission from many overlapping, relatively narrow lines of iron-group elements (IGEs), mostly Fe II, excited by the CSM interaction, in addition to strong  $H\alpha$  emission and often broad Ca II emission (e.g., Deng et al. 2004). Figure 13 shows spectra of PTF11kx and SN 2005gj, along with two comparison objects: SN 2010jl (a SN IIn; Smith et al. 2011b), and SN 1999aa (a somewhat overluminous SN Ia; Silverman et al. 2012a). The figure is reproduced from Silverman et al. (submitted) and some of the major spectral features are labeled.

We do not find strong evidence of oxygen in SNe Ia-CSM, which is often prominent in SNe IIn in the form of the O I  $\lambda 7774$  feature. However, it is possible that part of the very broad emission feature around 7400 Å (see especially Figures 1-5) is produced by O I  $\lambda 7774$

blended with [O II]  $\lambda\lambda 7319, 7330$ , along with the almost certain [Ca II]  $\lambda\lambda 7291, 7324$ . Moreover, note that the broad emission just blueward of  $H\alpha$  often seen in SNe Ia-CSM might be due to [O I]  $\lambda\lambda 6300, 6364$ , adding to the evidence for oxygen emission. However, it could more likely be related to the broad  $H\alpha$  emission underlying the narrower components discussed at length below.

To further investigate the spectral characteristics of SNe Ia-CSM (specifically as compared to SNe IIn), we measure properties of the  $H\alpha$ ,  $H\beta$ , and He I  $\lambda 5876$  features in all of the objects classified as SNe IIn from the Berkeley SN Group’s database (Silverman et al. 2012a) as well as the 63 SNe IIn discovered by PTF through August 2012. We follow the procedure of Dilday et al. (2012) and fit the spectral features with Gaussian profiles, using multiple components when necessary. In the following discussion, we are referring to the broader component with FWHM of about 500–2000 km s<sup>-1</sup>, unless otherwise specified. Furthermore, we found that the similarities and differences between SNe IIn and SNe Ia-CSM were relatively persistent at all epochs, and thus in the analysis below we consider data on *all* SNe IIn and SNe Ia-CSM at *all* epochs.

We find that SNe Ia-CSM tend to have  $H\alpha$  profiles which, for the most part, match the bulk of the SN IIn distribution. The velocity associated with the peak of



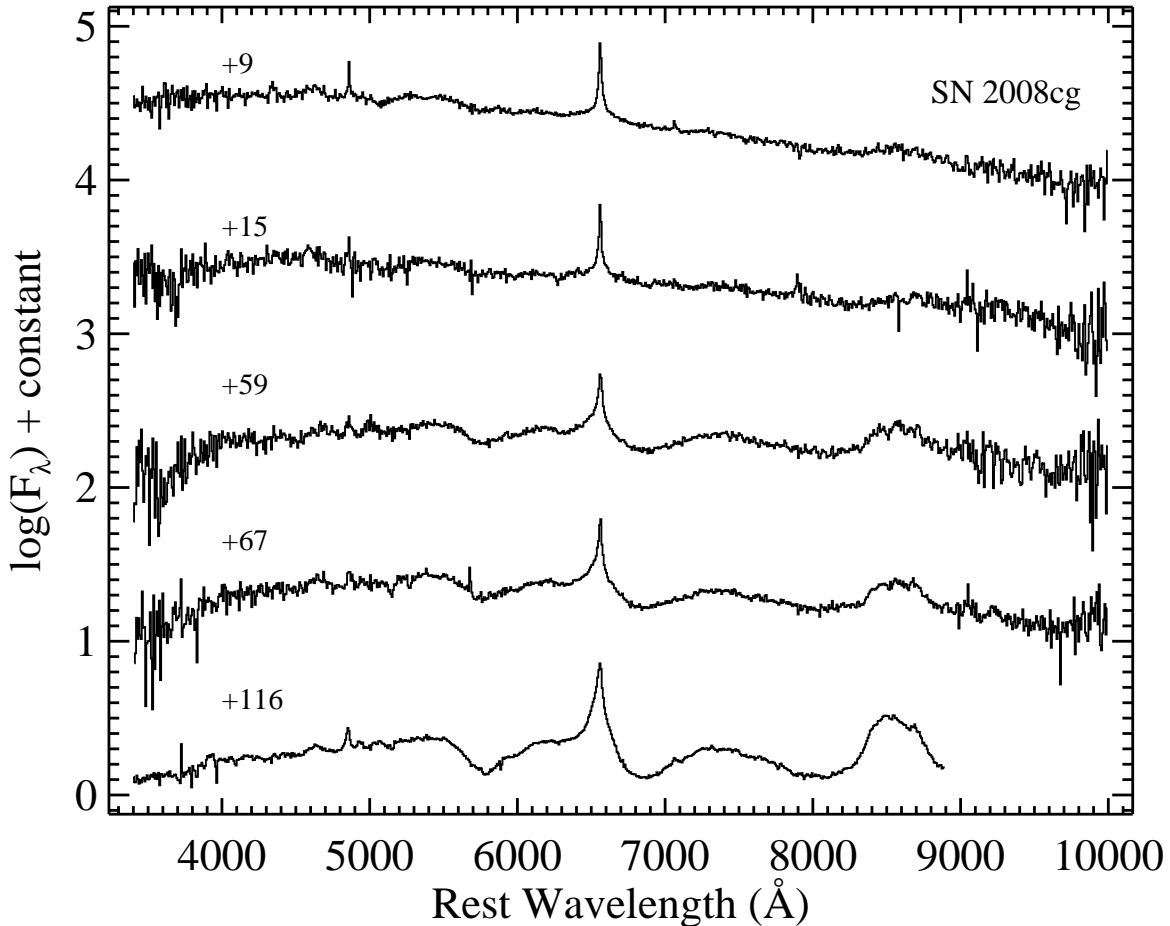


FIG. 4.— Spectra of SN 2008cg, the  $H\alpha$  profiles of which were analyzed by Fox et al. (2011), labeled with age relative to maximum brightness. The data have had their host-galaxy recession velocity removed and have been corrected for Galactic reddening.

the  $H\alpha$  emission in SNe Ia-CSM is slightly redshifted from the systemic velocity of their host galaxies, whereas the SN IIn peaks match their host-galaxy velocities more closely. However, this redshift is not statistically significant. Also, the equivalent width (EW) and FWHM of  $H\alpha$  are slightly smaller in SNe Ia-CSM as compared with SNe IIn, but again this is not a statistically significant result. For SNe Ia-CSM having multiple spectra, we find that the EW of  $H\alpha$  shows strong fluctuations until  $\sim 100$ – $150$  d past maximum brightness, perhaps indicating the SN ejecta are interacting with multiple CSM shells of varying sizes and/or densities. At later epochs, the EW tends to increase with time until  $\sim 1$  yr past maximum, when the EW possibly begins to decrease. This overall behavior has been seen previously in PTF11kx (Dilday et al. 2012; Silverman et al. submitted), SN 2002ic (Wang et al. 2004), and SN 2005gj (Aldering et al. 2006; Prieto et al. 2007).

The typical luminosities of  $H\alpha$  emission in nearly all of the SNe Ia-CSM studied herein (including PTF11kx) fall in the range  $(1\text{--}9)\times 10^{40}$  erg  $s^{-1}$ . The only object that lies outside this range is CSS120327:110520–015205 (which has a luminosity of  $\sim 3.9 \times 10^{41}$  erg  $s^{-1}$ ). Previously calculated  $H\alpha$  luminosities of SNe Ia-CSM are consistent with this range. Specifically, SN 2002ic had a luminosity of  $\sim 5 \times 10^{40}$  erg  $s^{-1}$  (Kotak et al. 2004), SN 2005gj

had luminosities of  $(1\text{--}10)\times 10^{40}$  erg  $s^{-1}$  (Aldering et al. 2006; Prieto et al. 2007), and SN 2008J had a luminosity of  $\sim 1.3 \times 10^{41}$  erg  $s^{-1}$  (Taddia et al. 2012).

In their respective references (and assuming shock velocities of a few thousand  $\text{km s}^{-1}$  and wind velocities of  $\sim 100$   $\text{km s}^{-1}$ ), the  $H\alpha$  luminosities of these three SNe Ia-CSM were converted into mass-loss rates in the range  $(2\text{--}120)\times 10^{-4}$   $M_{\odot}$   $\text{yr}^{-1}$ , which is quite a bit lower than the mass-loss rates we infer using the rise times of SNe Ia-CSM. This may be due to the fact that these estimates usually assume that the  $H\alpha$  emission is produced by optically thin CSM being ionized by the SN radiation field, whereas we will show below that the  $H\alpha$  feature is instead likely produced largely by collisional excitation.

In more typical SNe IIn (i.e., ones that almost certainly came from the core-collapse of a massive star), decreased flux in the red wing of  $H\alpha$  compared with the blue wing has been interpreted as a sign of new dust forming in the post-shock material (e.g. Fox et al. 2011; Smith et al. 2012). In fact, Fox et al. (2011) showed this exact phenomenon for SNe 2008J and 2008cg. Figures 14–16 display the  $H\alpha$  profiles of the 12 SNe Ia-CSM for which we present spectra in this paper. Following the method of Fox et al. (2011), we first remove a linear continuum near  $H\alpha$  from each spectrum (the long-dashed lines in the figures represent the now-horizontal continuum level). Next

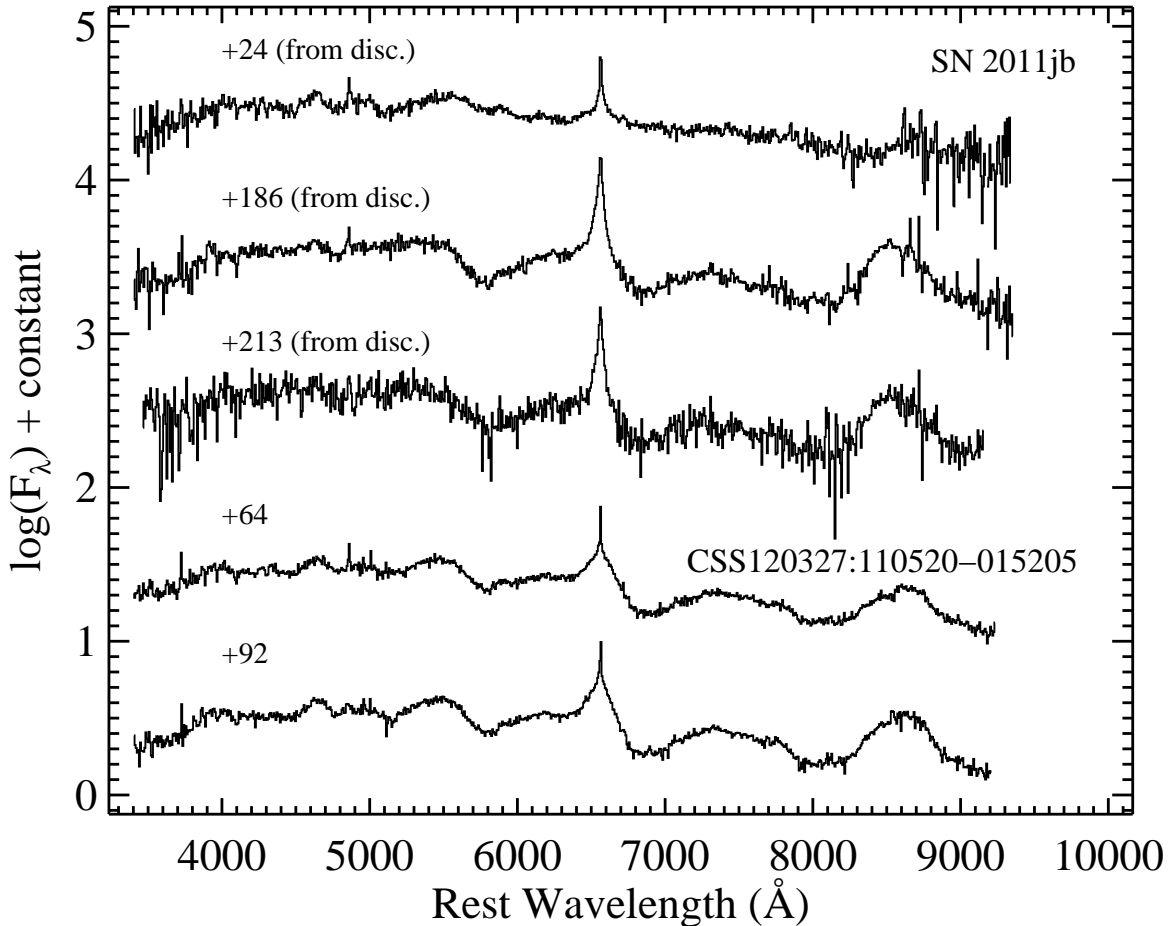


FIG. 5.— Spectra of SN 2011jb labeled with age relative to the discovery date and spectra of CSS120327:110520–015205 labeled with age relative to maximum brightness. The data have had their host-galaxy recession velocity removed and have been corrected for Galactic reddening.

we reflect the blue half of the  $H\alpha$  profile across the peak flux, yielding the short-dashed lines in the figures. The dotted vertical lines are the systemic velocity of each object.

We recover the result of Fox et al. (2011) that SNe 2008J and 2008cg both show diminished flux in the red wing of  $H\alpha$  compared with the blue wing. Surprisingly, we see the exact same behavior in nearly all of the other non-PTF SNe Ia-CSM at similar epochs. The red wings begin to decrease in flux at  $\sim 75$ – $100$  d past maximum brightness and seem to continue decreasing with time. We do note, however, that there is some evidence that the red flux in SN 2008J begins to increase again at the latest epochs covered by our spectra. We do not see this behavior in the PTF SNe Ia-CSM because we lack spectra at epochs later than  $\sim 75$  d past maximum brightness (except for one spectrum of PTF10iuf taken 86 d past maximum, which possibly shows evidence of a slight decrease in flux in the red wing of  $H\alpha$ , as does the spectrum of PTF11hcx taken 55 d past maximum). In Fox et al. (2011),  $10^{-3}$ – $10^{-2} M_{\odot}$  of dust was inferred from the mid-IR observations of SNe 2008J and 2008cg, but we caution that there are quite a few assumptions going into the conversion from mid-IR photometry to dust mass. Interestingly, PTF11kx does *not* show this evi-

dence for dust formation through 436 d past maximum brightness. However, there is some evidence of a decrease in the red wing of  $H\alpha$  in the spectrum from 680 d past maximum (Silverman et al. submitted).

In contrast to  $H\alpha$ , the EW of  $H\beta$  in SNe Ia-CSM is significantly smaller than that of normal SNe IIn. The median  $H\beta$  EW for SNe Ia-CSM is  $\sim 6$  Å, yet it is  $\sim 13$  Å for SNe IIn. Furthermore, the EW values of the two SN types seem to be drawn from different parent populations; a Kolmogorov-Smirnov (KS) test yields  $p \approx 0.0003$ . The top panel of Figure 17 shows the cumulative fraction of  $H\beta$  EWs for the SNe IIn from the Berkeley SN Group’s database as well as the SNe IIn from PTF. The SNe Ia-CSM with spectra presented in this work are represented by the red line while the SNe IIn are represented as the black line. The median EW was used when there were multiple EW measurements for a given object.

Similarly, we can calculate the  $H\alpha/H\beta$  intensity ratio (hereafter, the Balmer decrement) of the SNe IIn and SNe Ia-CSM, which is shown in the bottom panel of Figure 17. The Balmer decrement is only somewhat smaller in SNe IIn compared with SNe Ia-CSM ( $\sim 3$  versus  $\sim 5$ , respectively), but according to a KS test this is significant ( $p \approx 0.024$ ). The Balmer decrement in SNe Ia-CSM also

TABLE 6  
SPECTRA OF PTF SNe IA-CSM

UT Date	Age (d) <sup>a</sup>	Instrument <sup>b</sup>	Range (Å)	Res. (Å) <sup>c</sup>	Exp. (s)
PTF10htz					
2010 June 13.3	27	DBSP	3500–9800	3/4	450
2010 July 14.2	57	DBSP	3550–9900	3/4	450
PTF10iuf					
2010 June 7.1	–23	ISIS	3150–9500	3.5/7.2	900
2010 June 12.5	–19	LRIS	3258–10116	4.5/6.2	900
2010 July 7.4	3	LRIS	3300–10200	4.5/6	450
2010 Aug. 1.0	24	ISIS	3150–9500	3.5/7.2	900
2010 Aug. 8.3	30	DBSP	3400–9935	3/4	750
2010 Oct. 12.2	86	DEIMOS	4480–9630	3	750
PTF10yni					
2010 Nov. 3.2	3	RCS	3330–8235	5.9	1200
2010 Dec. 6.2	32	DBSP	3505–10000	3/4	600
2010 Dec. 13.2	38	DBSP	3500–9900	3/4	1200
PTF11dsb					
2011 June 2.1	17	LRIS	3040–10240	6.5/6	450
2011 July 5.4	45	DEIMOS	4592–7070	3	600
PTF11hzz					
2011 July 26.4	3	DBSP	3440–9800	3/4	900
2011 Aug. 1.5	8	DEIMOS	4765–9633	3	1000
2011 Aug. 6.4	12	DBSP	3400–9250	3/4	600
2011 Aug. 28.3	30	DBSP	3330–10000	3/4	430
2011 Sep. 29.4	56	DEIMOS	4583–8232	3	1200
PTF12efc					
2012 May 17.5	–23	LRIS	3382–10108	3.7/5.9	450
2012 May 22.4	–19	LRIS	3050–10257	6.5/6	480
2012 May 29.3	–14	DBSP	3480–10400	3/4	1200
2012 June 18.3	2	DBSP	3388–10120	3/4	1800
2012 July 16.3	25	DEIMOS	4500–8640	3	800
PTF12hnr					
2012 Aug. 9.5	2	Kast	3500–10000	4/10	2100
2012 Aug. 22.1	13	ISIS	3500–9476	3.5/7.2	1800

<sup>a</sup>Rest-frame days relative to maximum brightness, except for PTF11dsb and PTF12hnr where the epoch is relative to the date of discovery (2011 May 13 and 2012 Aug. 7, respectively). See Table 4 for the dates of maximum brightness for the rest of the objects.

<sup>b</sup>DBSP = Double Spectrograph on the Palomar 200 inch telescope; ISIS = Intermediate dispersion Spectrograph and Imaging System on the 4.2 m William Herschel Telescope; LRIS = Low Resolution Imaging Spectrometer on the Keck 10 m telescope; DEIMOS = DEep Imaging Multi-Object Spectrograph on the Keck 10 m telescope; RCS = RC Spec on the KPNO 4 m telescope; Kast = Kast double spectrograph on the Shane 3 m telescope at Lick Observatory.

<sup>c</sup>Approximate FWHM resolution. If two numbers are listed, they represent the blue-side and red-side resolutions, respectively.

appears to increase with time before eventually decreasing, peaking at ages anywhere from about a few months to a year and a half past maximum brightness. PTF11kx had  $H\alpha/H\beta > 7$  in all of its late-time spectra, and it too showed an increase and subsequent decrease, achieving a peak value at  $\sim 1$  yr past maximum brightness (Silverman et al. submitted). Furthermore, large Balmer decrements were also observed in SN 2005gj (Aldering et al. 2006).

A possible explanation for these large Balmer decrements is that the emission lines are produced primarily through collisional excitation rather than recombination. Recombination should lead to a Balmer decrement of  $\sim 3$ , while moderately high density gas can lead to large Balmer decrements when the optical depth of  $H\alpha$  is large (Drake & Ulrich 1980), possibly caused by Balmer self-absorption and collisional excitation (Xu et al. 1992). In SNe Ia-CSM, the SN ejecta may be interacting with thin, relatively dense, slowly moving shells of CSM that have cavities on either side of the shell, as one would expect from recurrent nova eruptions (and as was suggested for PTF11kx; Dilday et al. 2012). When the rapidly moving

SN ejecta catch up to and overtake the more slowly moving thin, dense shells, the hydrogen may get collisionally excited and naturally lead to the large  $H\alpha/H\beta$  ratios observed in the spectra of SNe Ia-CSM. Furthermore, models of SNe Ia-CSM interacting with a wind having a constant mass-loss rate appear to be inconsistent with late-time photometric observations (Chugai & Yungelson 2004). Thus, this relatively large Balmer decrement, which is ubiquitous in SNe Ia-CSM, is likely caused by interaction with multiple thin, dense shells of CSM.

The EW of He I  $\lambda 5876$  was relatively small in PTF11kx ( $\sim 9$  Å; Dilday et al. 2012; Silverman et al. submitted), smaller than that of most normal SNe IIn. Weak He I emission extends beyond just PTF11kx to the rest of the SNe Ia-CSM as well. Relatively narrow He I emission was detected in optical and near-IR spectra of SN 2008J taken a few days before maximum brightness, but the features were weak (Taddia et al. 2012). Figure 18 shows the cumulative fraction of EW of He I  $\lambda 5876$  for the Berkeley Group’s SNe IIn and the PTF SNe IIn in black, and for SNe Ia-CSM which have spectra shown in this work

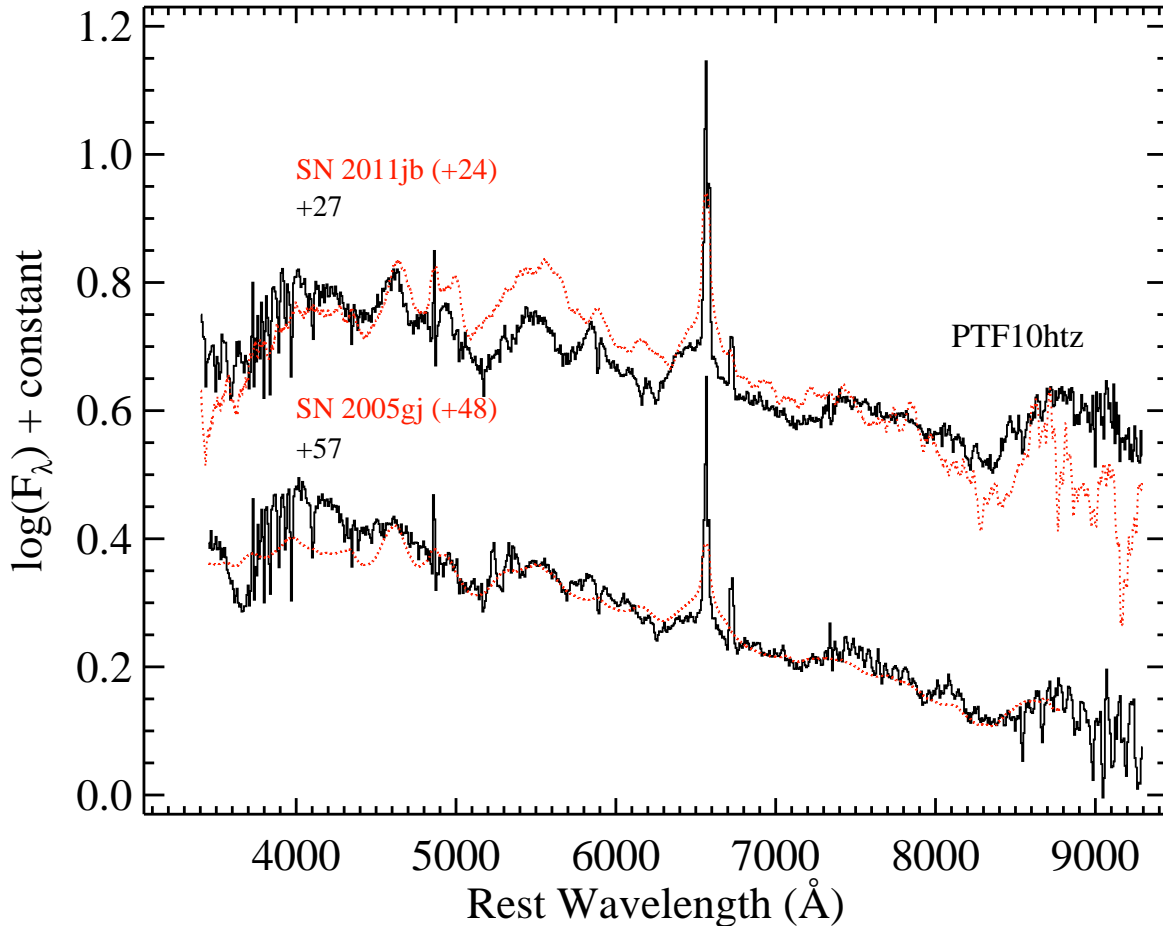


FIG. 6.— Spectra of PTF10htz labeled with age relative to maximum brightness, and a comparison spectrum (red). The data have had their host-galaxy recession velocity removed and have been corrected for Galactic reddening. Note that this object has a relatively large amount of host-galaxy contamination, but the superposed SN features match those of other SNe Ia-CSM quite well.

in red. The blue line is the SNe Ia-CSM, but including upper limits to the He I  $\lambda 5876$  EW, and the green line includes the upper limits for the *non*-SNe Ia-CSM. As above, the median EW is used when multiple EW measurements exist for a given object.

A KS test shows that the difference between SNe Ia-CSM and SNe IIn is significant ( $p \approx 0.009$ ), and the difference in median EW is striking ( $\sim 2$  Å versus  $\sim 6$  Å, respectively). Including the upper limits calculated for the EW of He I  $\lambda 5876$ , the difference is decreased (median EW values of  $\sim 2$  and  $\sim 4$  Å for SNe Ia-CSM and SNe IIn, respectively), and it is less significant ( $p \approx 0.017$ ). Thus, it seems that little to no He I emission is a common attribute of members of the SN Ia-CSM class. Perhaps the stronger He I emission in SNe IIn is due to an actual abundance enhancement in the wind from a massive star, as compared to the CSM shells coming from systems containing a WD (e.g., Chevalier & Fransson 1994).

As final note on optical spectroscopy of SNe Ia-CSM, we find that in most objects and at nearly all epochs the second strongest feature (after  $H\alpha$ ) is broad ( $\sim 10,000$  km s $^{-1}$ ) emission from the Ca II near-IR triplet. Every SN Ia-CSM discussed herein (with spectra that encompass this spectral feature near 8500–8600 Å) shows strong emission from the Ca II near-IR triplet (see Fig-

ures 1–11). The feature also appears prominently in late-time spectra of PTF11kx, though it almost completely disappears by 680 d past maximum brightness (Silverman et al. submitted). According to at least one model, this behavior may be the result of a cool, dense shell with separate Fe-poor and Fe-rich zones becoming fully mixed (Chugai et al. 2004).

#### 4.3. Other Observations of SNe Ia-CSM

In addition to optical photometry and low-resolution optical spectroscopy, there has been a smattering of other types of observations of SNe Ia-CSM at a variety of wavelengths. High-resolution optical spectra exist of relatively few SNe, and this is true of SNe Ia-CSM as well. However, for all SNe Ia-CSM with published high-resolution spectroscopy, narrow (50–100 km s $^{-1}$ ) P-Cygni profiles have been observed in  $H\alpha$ , as well as a handful of other spectral features (e.g., Kotak et al. 2004; Aldering et al. 2006; Dilday et al. 2012). Unfortunately, the spectra of SNe Ia-CSM presented herein are of such low resolution that we do not expect to observe these subtle features.

Weak, narrow Na I D absorption from the host galaxy of SN 2005gj was found in the high-resolution optical spectra presented by Aldering et al. (2006). On the other

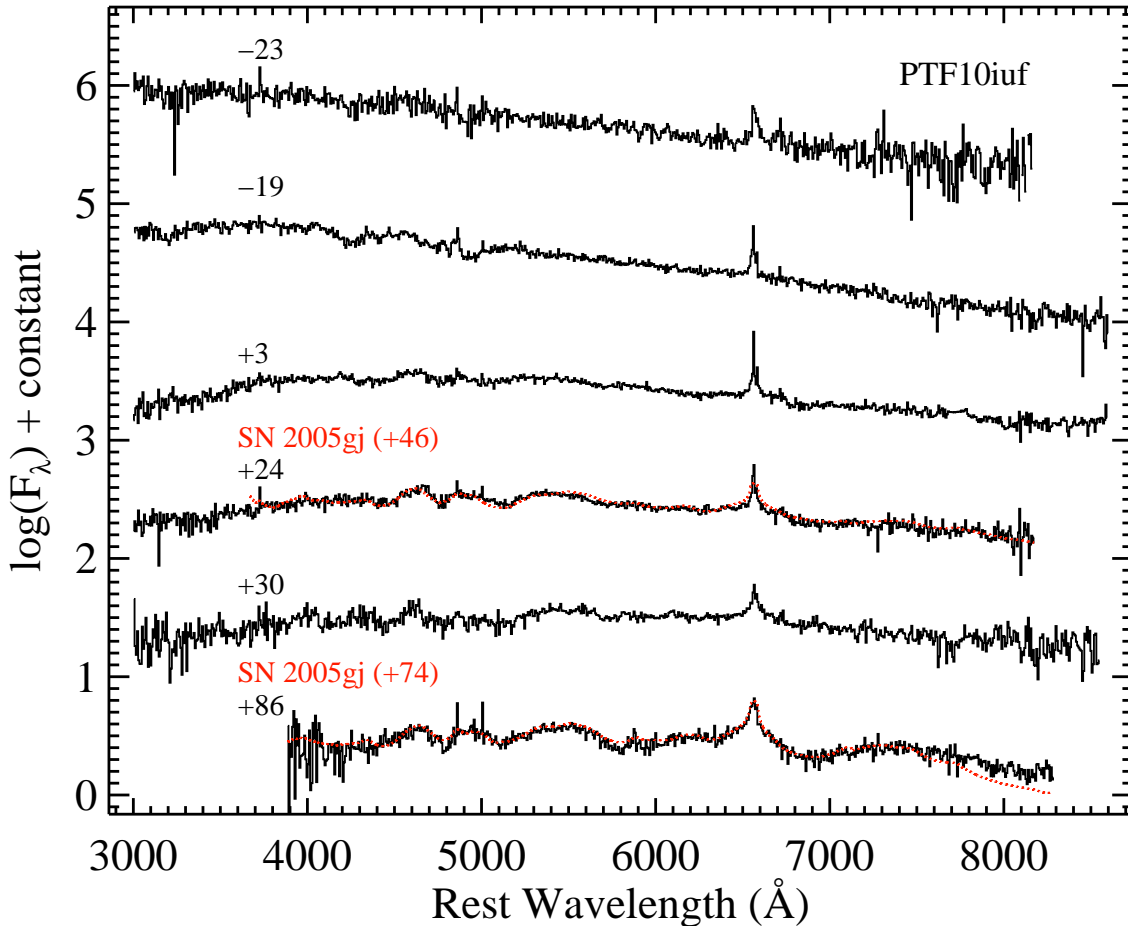


FIG. 7.— Spectra of PTF10iuf labeled with age relative to maximum brightness, and some comparison spectra (red). The data have had their host-galaxy recession velocity removed and have been corrected for Galactic reddening.

hand, Dilday et al. (2012) show strong Na I D absorption from the host galaxy of PTF11kx. Furthermore, a statistical study of many high-resolution optical spectra of SNe was undertaken by Sternberg et al. (2011), and the two SNe Ia-CSM in their sample (SNe 2008J and 2008cg, referred to as CCSNe) are found to have *saturated* Na I D lines, though the lines were redshifted in SN 2008J and blueshifted in SN 2008cg.

We inspect the low-resolution spectra presented in this work and find that all SNe Ia-CSM have likely Na I D absorption from the host galaxy. Regarding the two SNe Ia-CSM for which we do not present spectra herein, SN 1997cy probably does not show Na I D absorption from the host (Turatto et al. 2000; Germany et al. 2000), while SN 2002ic likely does (Benetti et al. 2006). Thus, narrow Na I D absorption from the host galaxy is present in nearly all SNe Ia-CSM.

High-resolution spectroscopy of SNe may be rare, but SN 2002ic is the only Ia-CSM object that has published spectropolarimetric observations. Wang et al. (2004) find that this object is mostly evenly polarized across the optical region at the  $\sim 0.8\%$  level, except near  $H\alpha$  where it is highly depolarized. They state that this is significantly different than more normal SNe Ia, and that in the case of SN 2002ic the polarization is likely more closely tied to the CSM than to the explosion itself.

At longer wavelengths than optical, we have already pointed out (in §2.3) that SNe 2008J and 2008cg are detected in the mid-IR by Fox et al. (2011). In fact, at  $\sim 620$  d past maximum brightness, SN 2008J is the second strongest IR detection in their study, with flux densities of 2.52 mJy and 2.71 mJy at  $3.6 \mu\text{m}$  and  $4.5 \mu\text{m}$ , respectively. While not as luminous, SN 2008cg at  $\sim 530$  d past maximum is also clearly detected with flux densities of 0.30 mJy and 0.35 mJy at  $3.6 \mu\text{m}$  and  $4.5 \mu\text{m}$ , respectively. The two best-studied SNe Ia-CSM are also found to have IR excesses at late times. SN 2002ic is easily detected in  $K$ -band imaging  $\sim 256$  d past maximum brightness as well as in  $H$ -band and  $K$ -band imaging  $\sim 352$  d past maximum (Kotak et al. 2004). From  $\sim 40$ – $140$  d past maximum, SN 2005gj is found to be 2–3 mag brighter and to decline more slowly than normal SNe Ia and SNe II in  $JHK_s$  imaging (Prieto et al. 2007). These IR excesses are consistent with the new dust formation scenario described above in order to explain the decreasing flux in the red wing of  $H\alpha$  at late times. In addition, there exists only one published near-IR spectrum (extending to  $2.2 \mu\text{m}$ ) of a Ia-CSM object (SN 2008J), and it shows emission lines of the H Paschen and Brackett series, along with likely Fe II emission and weak He I emission (Taddia et al. 2012).

Proceeding to even lower energy radiation, SN 1997cy

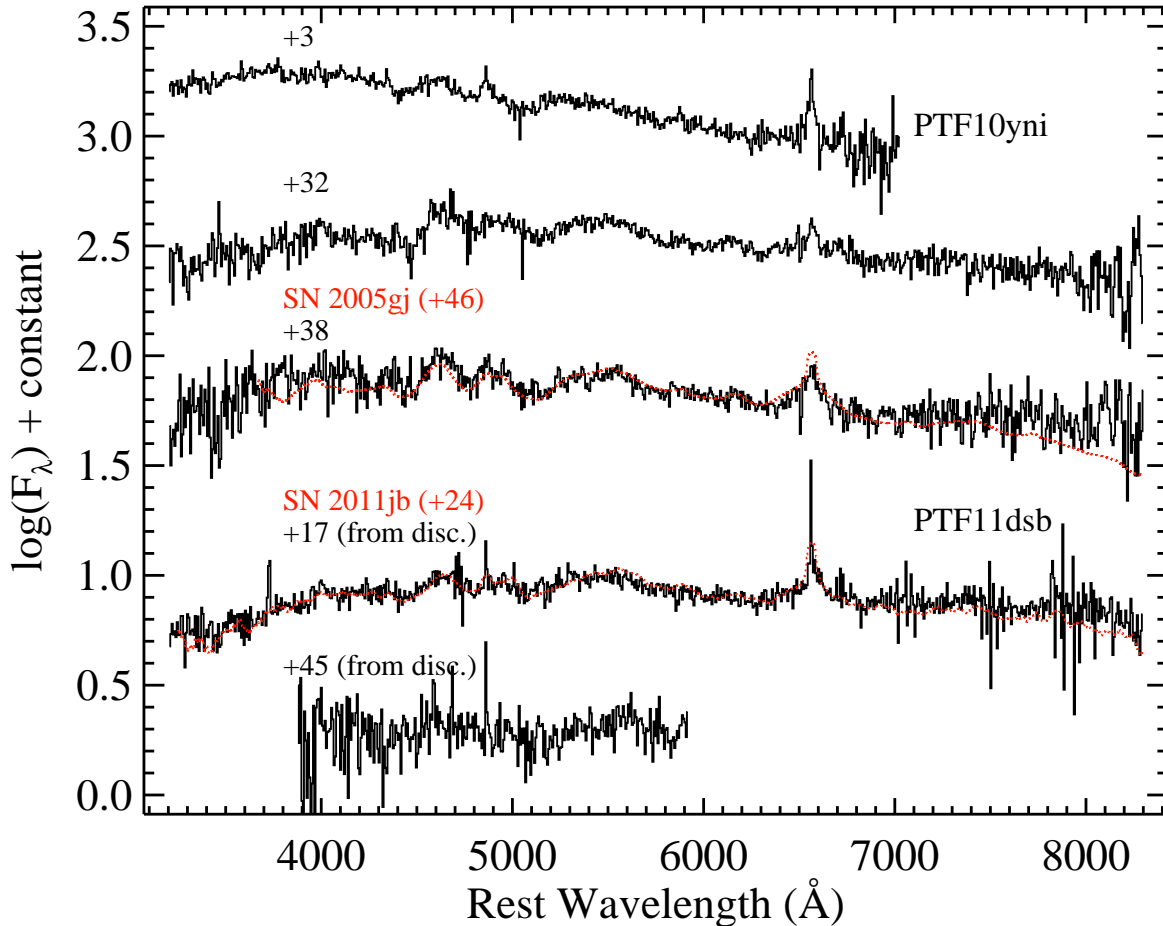


FIG. 8.— Spectra of PTF10yni labeled with age relative to maximum brightness and spectra of PTF11dsb labeled with age relative to the discovery date, and some comparison spectra (red). The data have had their host-galaxy recession velocity removed and have been corrected for Galactic reddening.

is not detected at 13 or 20 cm  $\sim 400$  d after discovery, though the limits ( $\sim 2 \times 10^{21}$  W Hz $^{-1}$ ) are not very restrictive (Germany et al. 2000). Similarly, neither SN 2005gj (at  $\sim 39$  d past maximum brightness; Soderberg & Frail 2005) nor SN 2008cg (at  $\sim 61$  d past maximum; Chandra & Soderberg 2008) are detected at 8.46 GHz with the Very Large Array. PTF12hnr, observed at 6.1 GHz using the EVLA  $\sim 20$  d after discovery, also resulted in a null detection. These observations can be converted into radio luminosity upper limits of  $\sim 10^{26}$ – $10^{28}$  erg s $^{-1}$  Hz $^{-1}$ . This range encompasses both upper limits and actual detections of more typical SNe IIn (e.g., Germany et al. 2000; Pooley et al. 2002; Fox et al. 2011).

At higher energies, both SN 2005gj (Immler et al. 2005) and SN 2008cg (Immler et al. 2008) are easily detected  $\sim 39$  and  $\sim 62$  d past maximum, respectively, by *Swift*/UVOT in the ultraviolet, including the bluest filter which covers 112–264 nm. PTF11hcx and PTF12efc, also observed by *Swift*/UVOT (the former  $\sim 9$  d after maximum brightness and the latter  $\sim 29$  and 16 d before maximum), are both well-detected in all observations.

Moving into the X-rays, SN 2005gj was not detected by *Swift*/XRT  $\sim 39$  d past maximum brightness (Immler et al. 2005) or by *Chandra*/ACIS  $\sim 55$  d past maximum (Prieto et al. 2007). Similarly, no detection of SN 2008cg

was made by *Swift*/XRT  $\sim 62$  d past maximum brightness (Immler et al. 2008). Unsurprisingly, PTF11hcx was also not detected by *Swift*/XRT  $\sim 9$  d after maximum brightness. The upper limits on the X-ray luminosity implied by these null detections are  $\sim 10^{39}$ – $10^{43}$  erg s $^{-1}$ ; observed X-ray fluxes of SNe IIn fall in this range (e.g., Pooley et al. 2002; Zampieri et al. 2005; Immler et al. 2007). Using the upper limits determined from the X-ray non-detections of SNe Ia-CSM and equations in Ofek et al. (2013), we calculate mass-loss rate upper limits of a few times  $10^{-1}$   $M_{\odot}$  yr $^{-1}$  (which matches the mass-loss rates calculated above using the rise times of SNe Ia-CSM).

#### 4.4. Host Galaxies of SNe Ia-CSM

Prieto et al. (2007) found that the host galaxies of the first four discovered SNe Ia-CSM (SNe 1997cy, 1999E, 2002ic, and 2005gj) are all late-type galaxies (dwarf irregulars and late-type spirals) with star formation likely occurring within the last few hundred Myr. They also show that, with the exception of the host of SN 1999E, the hosts have low luminosities ( $-19.1 < M_r < -17.6$  mag, similar to the Magellanic clouds) which implies subsolar metallicities. The host of SN 1999E, however, is bright in the IR, shows a nuclear starburst, but is consistent with solar metallicity and Milky Way (MW) luminosity

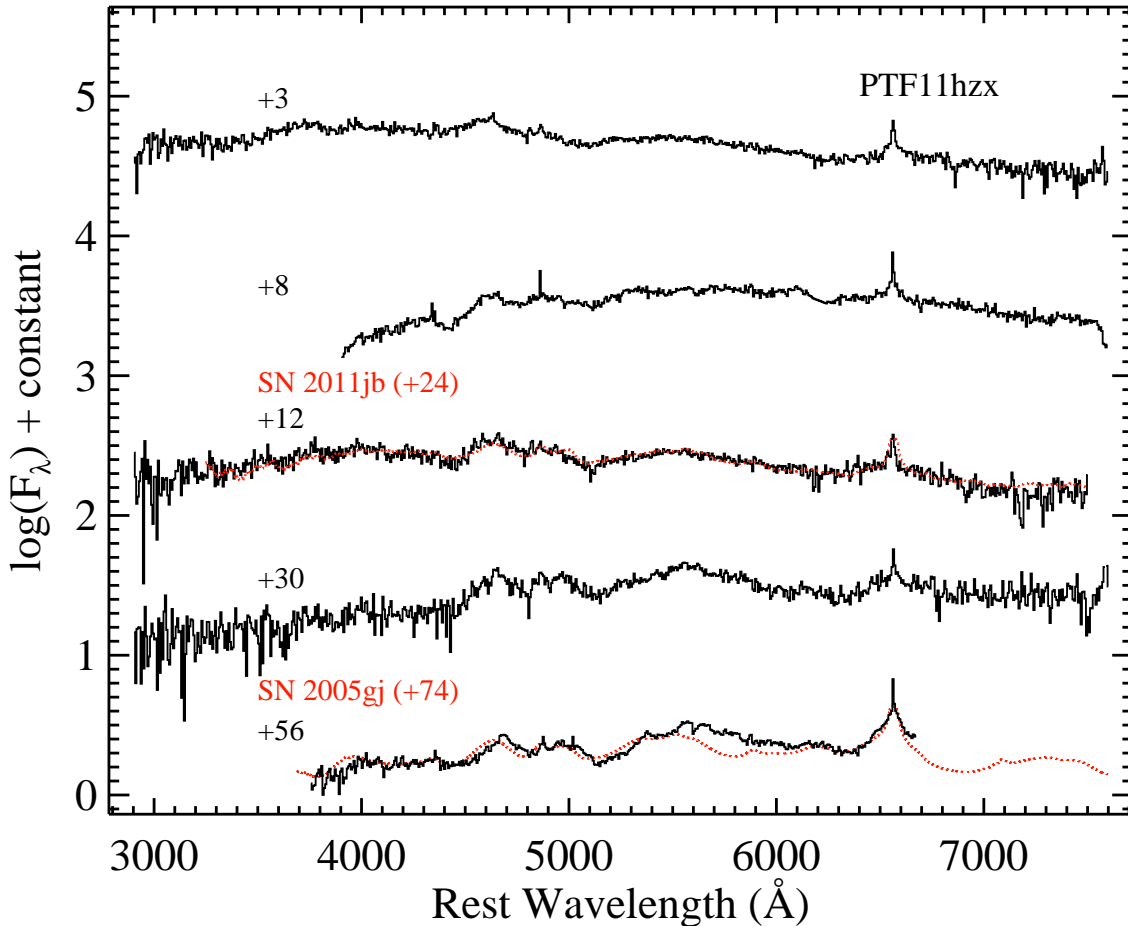


FIG. 9.— Spectra of PTF11hzx labeled with age relative to maximum brightness, and some comparison spectra (red). The data have had their host-galaxy recession velocity removed and have been corrected for Galactic reddening.

(Allen et al. 1991; Prieto et al. 2007).

Using the NASA/IPAC Extragalactic Database (NED) and the Sloan Digital Sky Survey Data Release 8 (SDSS DR8; Aihara et al. 2011), we find that the hosts of the four other non-PTF SNe Ia-CSM discussed in this work are also late-type galaxies. Three of the four have relatively low luminosities ( $-19.3 < M_r < -18.1$  mag), while the host of SN 2008J appears to be consistent with MW luminosity (much like the host of SN 1999E).

Turning now to the PTF SNe Ia-CSM, PTF11kx has a late-type spiral host with luminosity comparable to that of the MW and slightly higher-than-solar metallicity (Dilday et al. 2012; Tremonti et al. 2004). Four of the seven newly discovered SNe Ia-CSM in PTF (PTF10htz, PTF10iuf, PTF11dsb, and PTF12hnr) are also found in what are likely late-type spiral hosts, all of which have luminosities similar to that of the MW ( $-20.6 < M_r < -19.2$  mag). The remaining three PTF SNe Ia-CSM (PTF10yni, PTF11hzx, and PTF12efc) do not have detectable hosts in SDSS DR8 (Aihara et al. 2011) or in our deep stacks of PTF search images. This implies that they are low-luminosity galaxies with  $M_r \gtrsim -18$  mag.

Thus, of the 16 SNe Ia-CSM discussed herein, all appear to have exploded in late-type galaxies. Nine of them are found in low-luminosity (and presumably, low-metallicity) hosts, including three hosts that are not de-

tected by SDSS DR8 or PTF, while seven of them (including PTF11kx) are found in hosts roughly similar to the MW. Interestingly, when the hosts of PTF SNe Ia-CSM are compared to the hosts of SNe IIn from PTF, no significant differences are found. It has been shown in earlier work that SNe II in general have statistically the same hosts as SNe IIn (Kelly & Kirshner 2012), and that SNe IIn and SNe IIP both trace recent (but not ongoing) star formation (Anderson et al. 2012). Furthermore, contrary to some expectations, Anderson et al. (2012) find that SNe IIn do not come from the youngest (and thus most massive) stars; instead, their progenitors are slightly older than those of SNe IIP. They also find that the association with host-galaxy  $H\alpha$  emission for SNe IIn is between that of other SNe II and SNe Ia, perhaps implying that some of their SNe IIn are actually SNe Ia-CSM which have lower-mass progenitors than any CCSN subtype.<sup>25</sup>

## 5. CONCLUSIONS

Running SNID on the Berkeley SN Group’s database of SN IIn spectra, we have reidentified four SNe Ia-CSM that were previously known (SNe 2008J, 2008cg,

<sup>25</sup> Note that none of the SNe Ia-CSM discussed herein were part of the Anderson et al. (2012) sample.



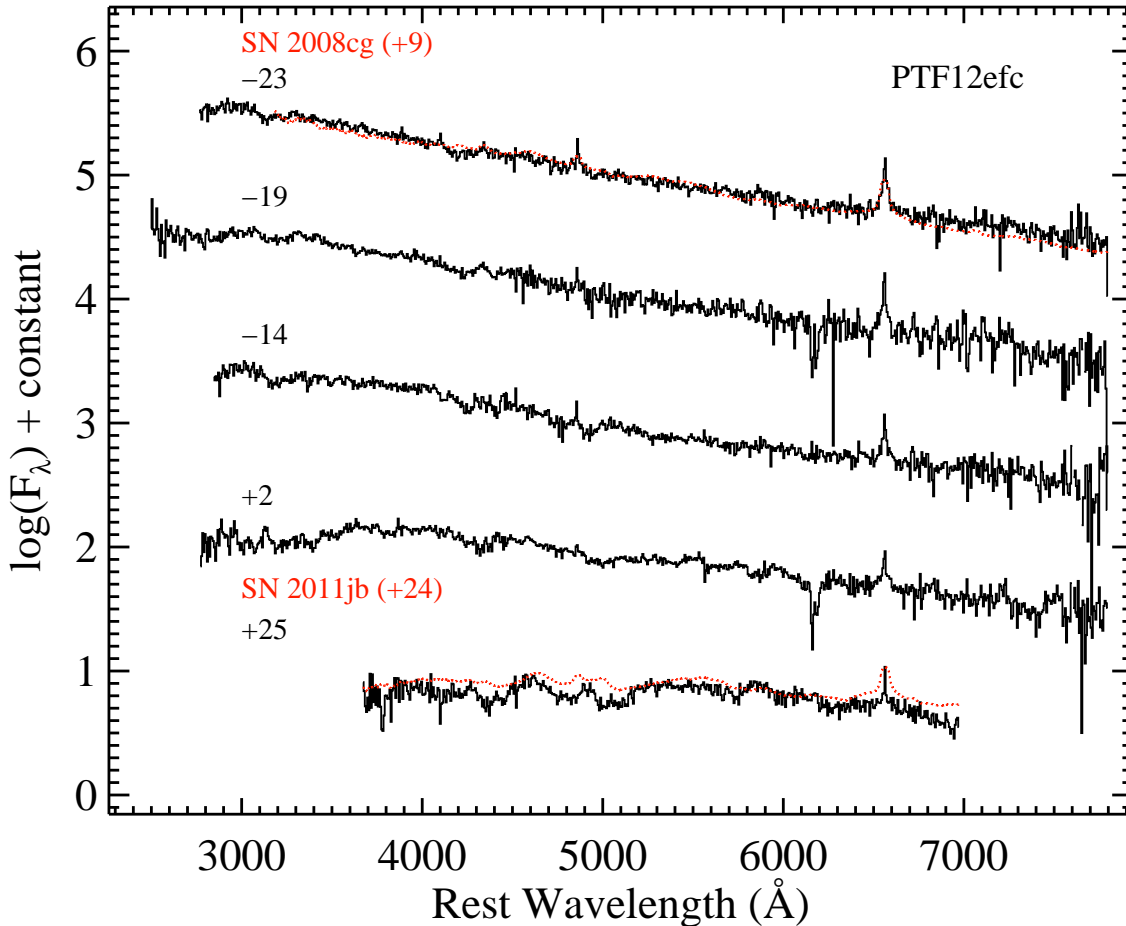


FIG. 10.— Spectra of PTF12efc labeled with age relative to maximum brightness, and some comparison spectra (red). The data have had their host-galaxy recession velocity removed and have been corrected for Galactic reddening.

2011jb, and CSS120327:110520–015205) but poorly studied. These are in addition to the four well-studied Ia-CSM objects (SNe 1997cy, 1999E, 2002ic, and 2005gj). Furthermore, SNID was run on all 63 SNe IIn discovered by PTF through August 2012, and seven new SNe Ia-CSM were uncovered. Armed with a sample of 15 SNe Ia-CSM, in addition to PTF11kx (Dilday et al. 2012; Silverman et al. submitted), we investigate the unifying characteristics of this class of SN. Observable signatures of SNe Ia-CSM are as follows.

- Peak absolute magnitudes of  $-21.3 \leq M_R \leq -19$  mag are observed (somewhat more luminous than normal SNe Ia and the bulk of the SNe IIn population, but less luminous than superluminous SNe) and relatively long rise times of  $\sim 20$ – $40$  d (as opposed to  $\sim 18$  d for more normal SNe Ia).
- SNID cross-correlations of optical spectra show that SNe Ia-CSM are spectroscopically homogeneous. The spectra consist of a diluted SN Ia spectrum, along with a relatively blue “quasi-continuum” from many blended lines of IGEs, strong and broad ( $\sim 10,000$  km s $^{-1}$ ) emission from the Ca II near-IR triplet, and are dominated by H $\alpha$  emission with widths of  $\sim 2000$  km s $^{-1}$ .
- The H $\alpha$  profile shows strong fluctuations until  $\sim 100$ – $150$  d past maximum brightness, at which time the strength tends to increase with time. There are also extremely narrow ( $50$ – $100$  km s $^{-1}$ ) P-Cygni profiles present in H $\alpha$ , and after  $\sim 75$ – $100$  d past maximum a decrease in flux in the red wing is seen (often attributed to newly formed dust).
- Weak He I and H $\beta$  emission are seen, as compared to typical SNe IIn, and the H $\alpha$ /H $\beta$  intensity ratio is large. This is likely caused by collisional excitation of hydrogen when the SN Ia-CSM ejecta overtake slower-moving, thin, moderately dense CSM shells.
- Within the first few months after explosion, ultraviolet emission is seen, but no radio or X-ray emission is detected (although the range of upper limits derived is consistent with both upper limits and actual detections of SNe IIn at radio and X-ray wavelengths). Mid-IR emission is visible at  $\sim 0.5$ – $2$  yr past maximum brightness, and it is stronger than in typical SNe IIn or SNe Ia (which is further evidence of newly formed dust).
- Using both rise times and X-ray upper limits, SNe Ia-CSM seem to have mass-loss rates of a few times  $10^{-1}$  M $_{\odot}$  yr $^{-1}$ , though we caution that there



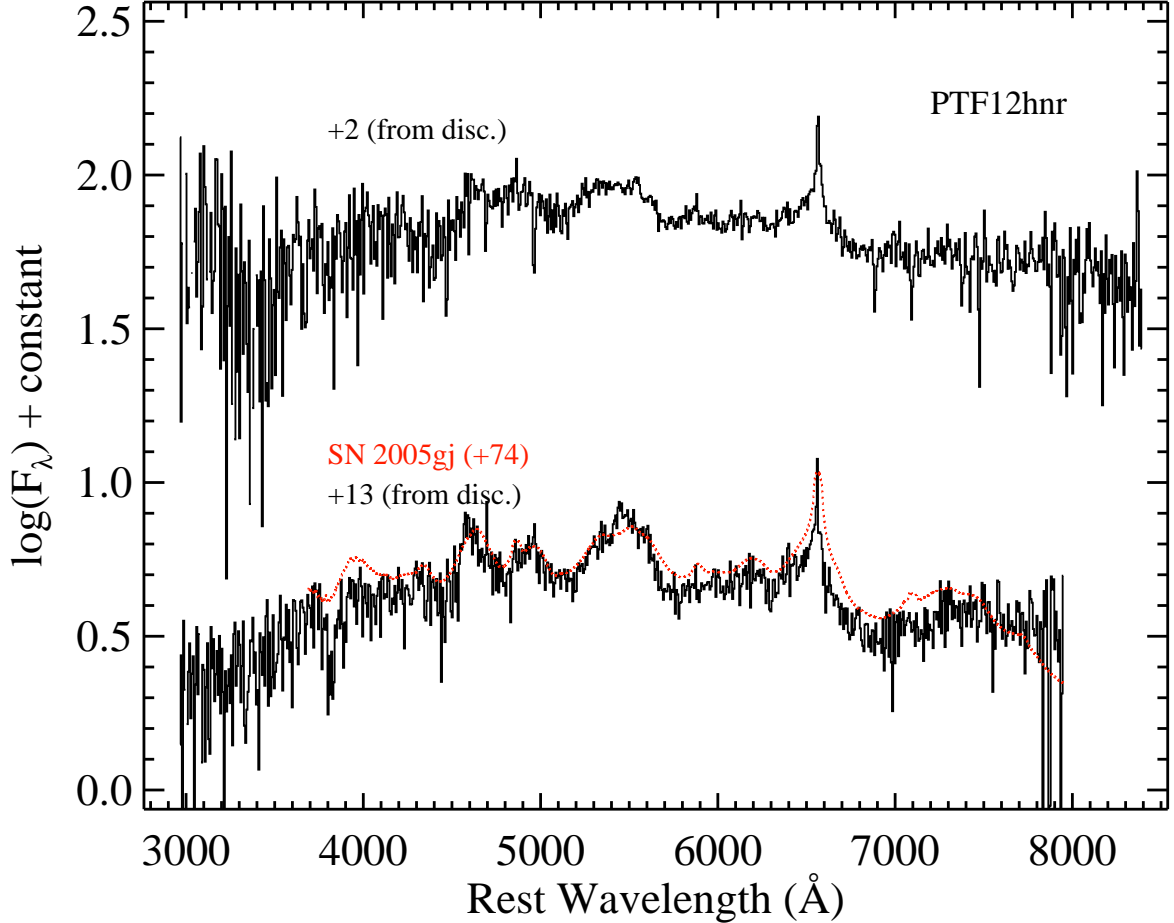


FIG. 11.— Spectra of PTF12hr labeled with age relative to the discovery date, and some comparison spectra (red). The data have had their host-galaxy recession velocity removed and have been corrected for Galactic reddening.

are many assumptions that go into these calculations.

- The hosts of SNe Ia-CSM all appear to be late-type spirals with either MW-like luminosities (and solar metallicities) or dwarf irregulars having luminosities similar to those of the Magellanic Clouds (and thus presumably subsolar metallicities).

While the above list describes attributes of the Ia-CSM objects, several of the items can also describe more typical SNe IIn. This brings up the possibility, noted previously (e.g., Anderson et al. 2012), that some subset of the SN IIn population is contaminated by SNe Ia-CSM. Perhaps there are simply some *bona fide* SNe IIn that share with SNe Ia-CSM many, but not all, of the observational characteristics listed above. It is also plausible that some SNe IIn that can be described by many of the items listed above are, in fact, SNe Ia-CSM where the CSM interaction is too strong or begins too early for any hint of an underlying SN Ia to be identified. On the other hand, at least *some* SNe IIn are actual core-collapse events since a massive progenitor star is detected (e.g., SN 2005gl; Gal-Yam & Leonard 2009).

The existence of the SN Ia-CSM class of objects seems to argue that at least some SNe Ia arise from the SD channel, since a H-rich CSM is likely a result of that

progenitor scenario (but see Shen et al. 2013). Detailed modeling of both the core collapse of massive stars and the thermonuclear explosion of WDs (with an assortment of binary companions) within various arrangements of CSM is beyond the scope of this paper, but we hope that future theoretical work on this subject will be informed by the observational results presented herein.

We would like to thank K. Alatalo, T. Barlow, E. Bellm, B. Cobb, A. Cucchiara, M. Ganeshalingam, Y. Green, M. Hidas, L. Kewley, N. Konidaris, S. Lazarevic, N. Lee, D. Levitan, M. McCourt, K. Mooley, R. Mostardi, D. Perley, A. G. Riess, B. Sesar, R. Street, T. Treu, V. Viscomi, and X. Wang for their assistance with some of the observations and data reduction; B. Dilday, O. Fox, and L. Wang for helpful discussions; and D. Balam, M. Stritzinger, J. Vinko, and J. C. Wheeler for providing unpublished spectra of possible SNe Ia-CSM. We are grateful to the staffs at the Isaac Newton Group of Telescopes and the Lick, Keck, Palomar, and Kitt Peak National Observatories for their support. Some of the data presented herein were obtained at the W. M. Keck Observatory, which is operated as a scientific partnership among the California Institute of Technology, the University of California, and the National Aeronautics

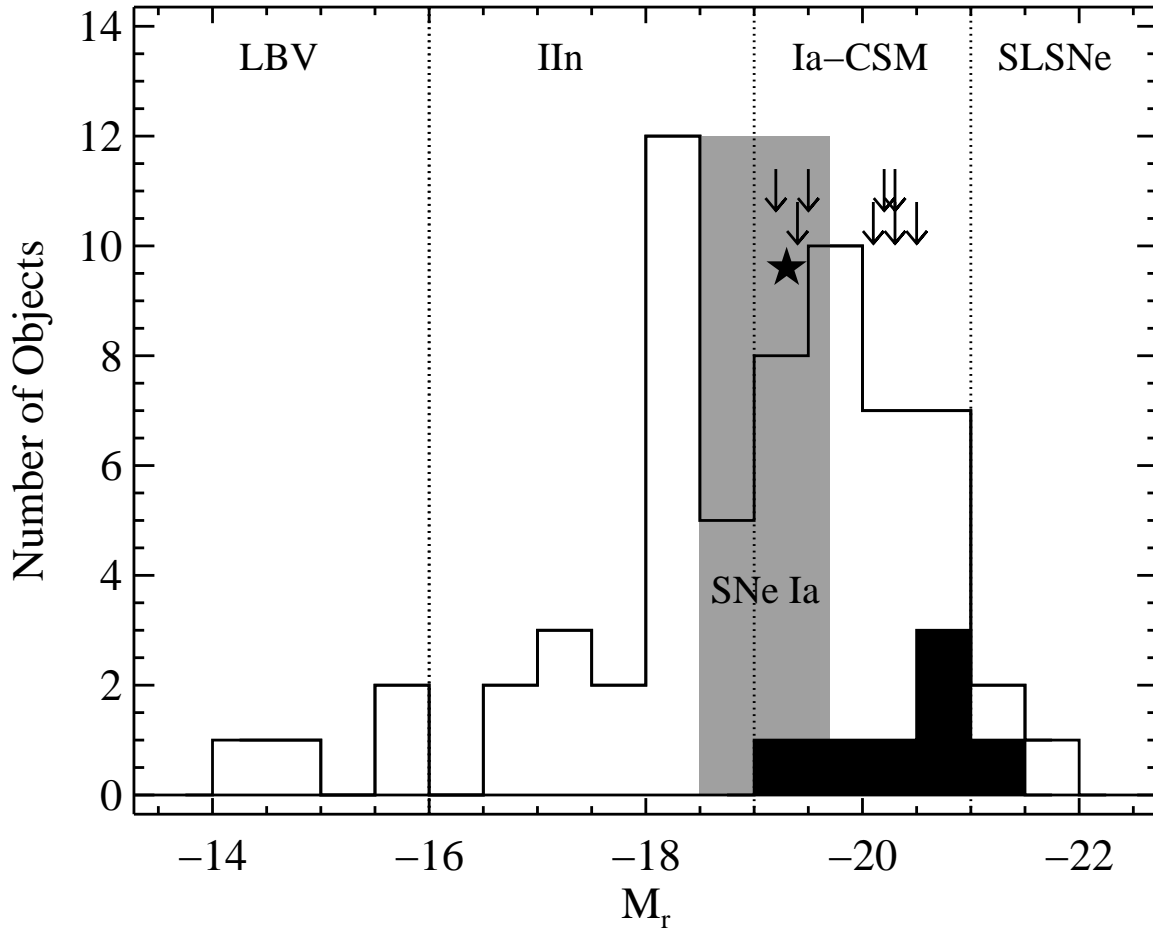


FIG. 12.— Peak absolute  $r$ -band magnitude of all 63 SNe IIn discovered by PTF through August 2012. The vertical dotted lines denote the boundaries between the various subtypes of SNe IIn and SNe Ia-CSM, and the gray shaded region is the range of SNe Ia that follow the Phillips relation. The black, filled histogram shows the seven SNe Ia-CSM discovered by PTF (not including PTF11kx), the downward-pointing arrows are the eight previously known SNe Ia-CSM, and the star is PTF11kx.

and Space Administration (NASA); the observatory was made possible by the generous financial support of the W. M. Keck Foundation. The authors wish to recognize and acknowledge the very significant cultural role and reverence that the summit of Mauna Kea has always had within the indigenous Hawaiian community; we are most fortunate to have the opportunity to conduct observations from this mountain. This research has made use of the NASA/IPAC Extragalactic Database (NED) which is operated by the Jet Propulsion Laboratory, California Institute of Technology, under contract with NASA. Funding for SDSS-III has been provided by the Alfred P. Sloan Foundation, the Participating Institutions, the

National Science Foundation, and the U.S. Department of Energy Office of Science. The SDSS-III web site is <http://www.sdss3.org/>. Supernova research by A.V.F.'s group at U.C. Berkeley is supported by Gary and Cynthia Bengier, the Richard and Rhoda Goldman Fund, the Christopher R. Redlich Fund, the TABASGO Foundation, and NSF grants AST-0908886 and AST-1211916. Work by A.G.-Y. and his group is supported by grants from the ISF, BSF, GIF, Minerva, an FP7/ERC grant, and the Helen and Martin Kimmel Award for Innovative Investigation. M.M.K. acknowledges generous support from a Hubble Fellowship and a Carnegie-Princeton Fellowship.

#### REFERENCES

- Aihara, H. et al. 2011, *ApJS*, 195, 26  
 Aldering, G. et al. 2006, *ApJ*, 650, 510  
 Allen, D. A., Norris, R. P., Meadows, V. S., & Roche, P. F. 1991, *MNRAS*, 248, 528  
 Anderson, J. P., Habergham, S. M., James, P. A., & Hamuy, M. 2012, *MNRAS*, 424, 1372  
 Arcavi, I. et al. 2010a, *ATel*, 3027, 1  
 —. 2010b, *ATel*, 2685, 1  
 Benetti, S., Cappellaro, E., Turatto, M., Taubenberger, S., Harutyunyan, A., & Valenti, S. 2006, *ApJ*, 653, L129  
 Blondin, S. & Calkins, M. 2008, *CBET*, 1363, 1  
 Blondin, S. & Tonry, J. L. 2007, *ApJ*, 666, 1024  
 Blondin, S. et al. 2009, *ApJ*, 693, 207  
 Bloom, J. S. et al. 2012, *ApJ*, 744, L17  
 Brown, P. J. et al. 2012, *ApJ*, 753, 22  
 Chandra, P. & Soderberg, A. 2008, *ATEL*, 1594, 1  
 Chevalier, R. A. & Fransson, C. 1994, *ApJ*, 420, 268  
 Chugai, N. N., Chevalier, R. A., & Lundqvist, P. 2004, *MNRAS*, 355, 627  
 Chugai, N. N. & Yungelson, L. R. 2004, *Astronomy Letters*, 30, 65

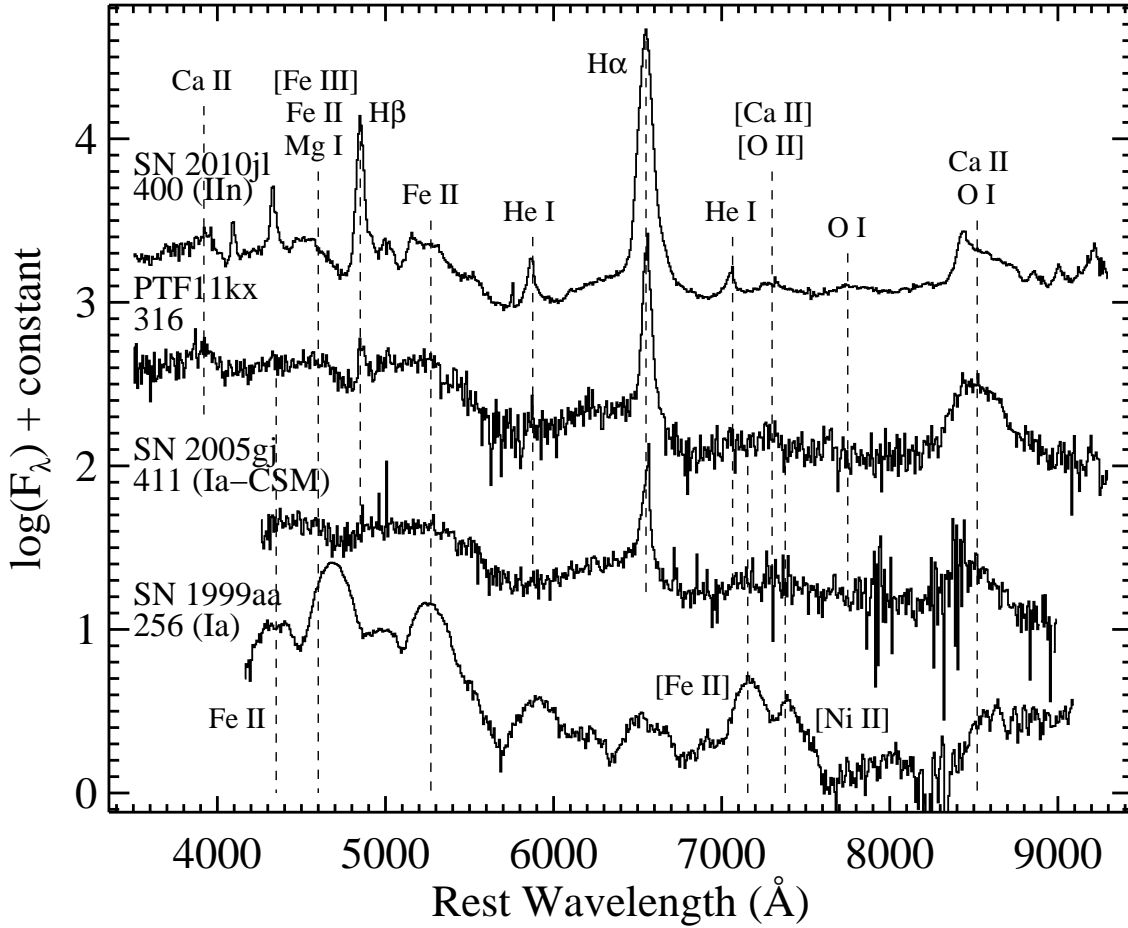


FIG. 13.— Spectra of PTF11kx and SN 2005gj, in addition to SN 2010jl (a SN II; Smith et al. 2011b) and SN 1999aa (a somewhat overluminous SN Ia; Silverman et al. 2012a). Each spectrum is labeled with its rest-frame age relative to maximum brightness and major spectral features are labeled. The data have had their host-galaxy recession velocity removed and have been corrected for Galactic reddening. The figure is reproduced from Silverman et al. (submitted).

- Deng, J., Kawabata, K. S., Ohya, Y., Nomoto, K., Mazzali, P. A., Wang, L., Jeffery, D. J., Iye, M., Tomita, H., & Yoshii, Y. 2004, *ApJ*, 605, L37
- Dilday, B. et al. 2012, *Science*, 337, 942
- Drake, A. J. et al. 2010, *ATel*, 2978, 1
- . 2012, *ATel*, 4081, 1
- Drake, S. A. & Ulrich, R. K. 1980, in *Bulletin of the American Astronomical Society*, Vol. 12, *Bulletin of the American Astronomical Society*, 798
- Filippenko, A. V. 1997, *ARA&A*, 35, 309
- Filippenko, A. V. 2000, in *American Institute of Physics Conference Series*, Vol. 522, *American Institute of Physics Conference Series*, ed. S. S. Holt & W. W. Zhang, 123–140
- Filippenko, A. V., Silverman, J. M., Mostardi, R., & Griffith, C. V. 2008, *CBET*, 1420, 1
- Foley, R. J. et al. 2012a, *ApJ*, 752, 101
- . 2012b, *ApJ*, 744, 38
- Fox, O. D. et al. 2011, *ApJ*, 741, 7
- Gal-Yam, A. 2012, *Science*, 337, 927
- Gal-Yam, A. & Leonard, D. C. 2009, *Nature*, 458, 865
- Gal-Yam, A. et al. 2011, *ATel*, 3403, 1
- Ganeshalingam, M., Li, W., & Filippenko, A. V. 2011, *MNRAS*, 416, 2607
- Ganeshalingam, M. et al. 2010, *ApJS*, 190, 418
- Garavini, G. et al. 2004, *AJ*, 128, 387
- Germany, L. M., Reiss, D. J., Sadler, E. M., Schmidt, B. P., & Stubbs, C. W. 2000, *ApJ*, 533, 320
- Hamuy, M. et al. 2003, *Nature*, 424, 651
- Howell, D. A. 2011, *Nature Communications*, 2
- Howell, D. A. et al. 2006, *Nature*, 443, 308
- Iben, Jr., I. & Tutukov, A. V. 1984, *ApJS*, 54, 335
- Immler, S., Brown, P. J., Filippenko, A. V., & Pooley, D. 2007, *ATEL*, 1290, 1
- Immler, S., Filippenko, A. V., & Pooley, D. 2008, *ATEL*, 1598, 1
- Immler, S., Petre, R., & Brown, P. 2005, *IAU Circ.*, 8633, 2
- Kankare, E., Mattila, S., & Pastorello, A. 2011, *CBET*, 2947, 2
- Kelly, P. L. & Kirshner, R. P. 2012, *ApJ*, 759, 107
- Kiewe, M. et al. 2012, *ApJ*, 744, 10
- Kotak, R., Meikle, W. P. S., Adamson, A., & Leggett, S. K. 2004, *MNRAS*, 354, L13
- Law, N. M. et al. 2009, *PASP*, 121, 1395
- Li, W., Filippenko, A. V., Treffers, R. R., Riess, A. G., Hu, J., & Qiu, Y. 2001, *ApJ*, 546, 734
- Li, W. et al. 2011, *MNRAS*, 412, 1441
- Moore, K. & Bildsten, L. 2012, *ApJ*, 761, 182
- Nugent, P. E. et al. 2011, *Nature*, 480, 344
- Ofek, E. O. et al. 2012a, *PASP*, 124, 62
- . 2012b, *PASP*, 124, 854
- . 2013, *Nature*, 494, 65
- Patat, F. et al. 2007, *Science*, 317, 924
- Peek, J. E. G. & Graves, G. J. 2010, *ApJ*, 719, 415
- Phillips, M. M. 1993, *ApJ*, 413, L105
- Pooley, D. et al. 2002, *ApJ*, 572, 932
- Prieto, J. L. et al. 2007, *AJ*, submitted (arXiv: 0706.4088)
- Quimby, R. M., Yuan, F., Akerlof, C., & Wheeler, J. C. 2013, *MNRAS*, accepted (arXiv:1302.0911)
- Rau, A. et al. 2009, *PASP*, 121, 1334
- Rigon, L. et al. 2003, *MNRAS*, 340, 191
- Scalzo, R. A. et al. 2010, *ApJ*, 713, 1073
- Schlegel, D. J., Finkbeiner, D. P., & Davis, M. 1998, *ApJ*, 500, 525

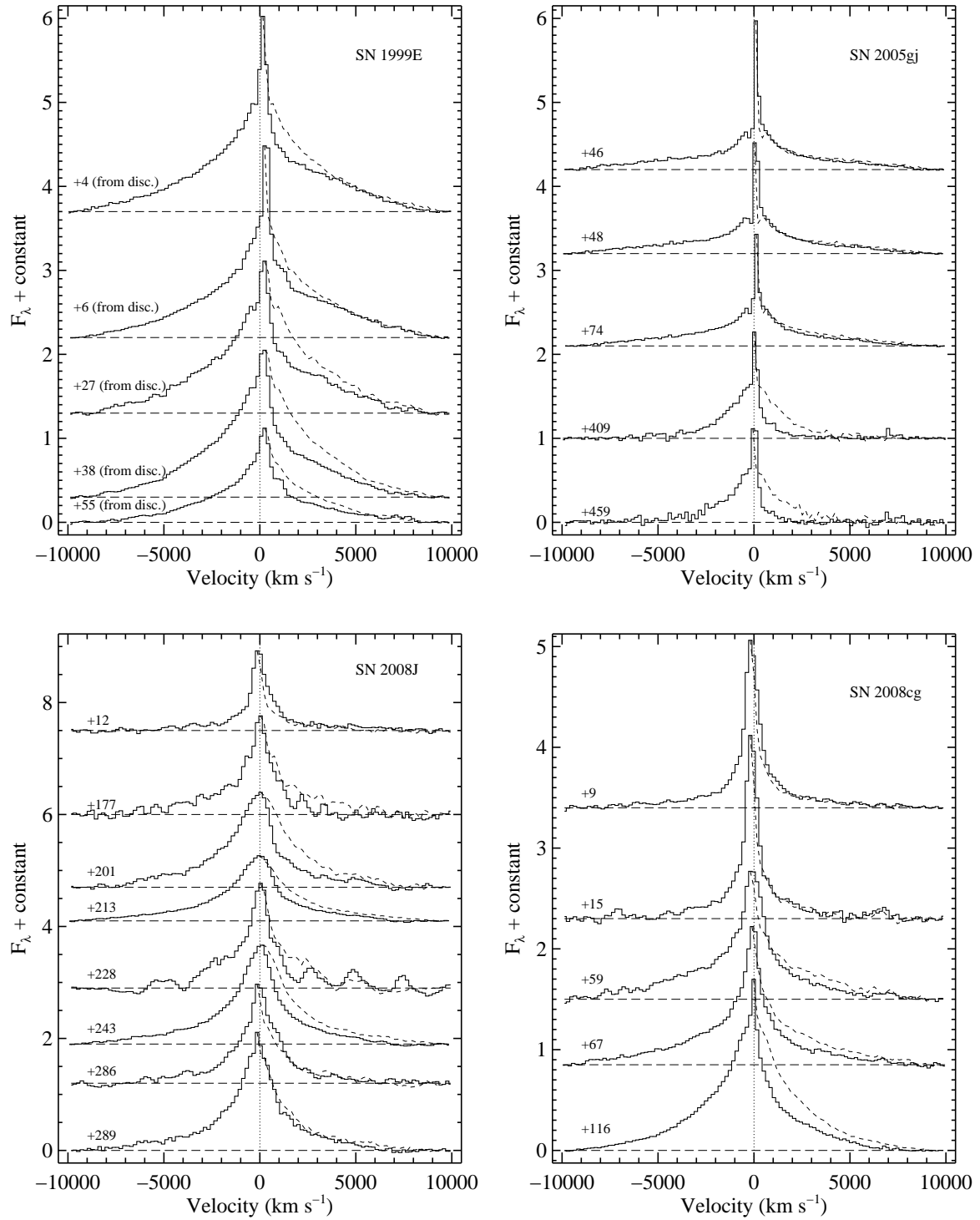


FIG. 14.— The H $\alpha$  profiles of SNe 1999E, 2005gj, 2008J, and 2008cg. After removing a linear continuum (the long-dashed lines represent the now-horizontal continuum level), we reflect the blue half of the H $\alpha$  profile across the peak flux, yielding the short-dashed lines. The dotted vertical line is the systemic velocity of each object.

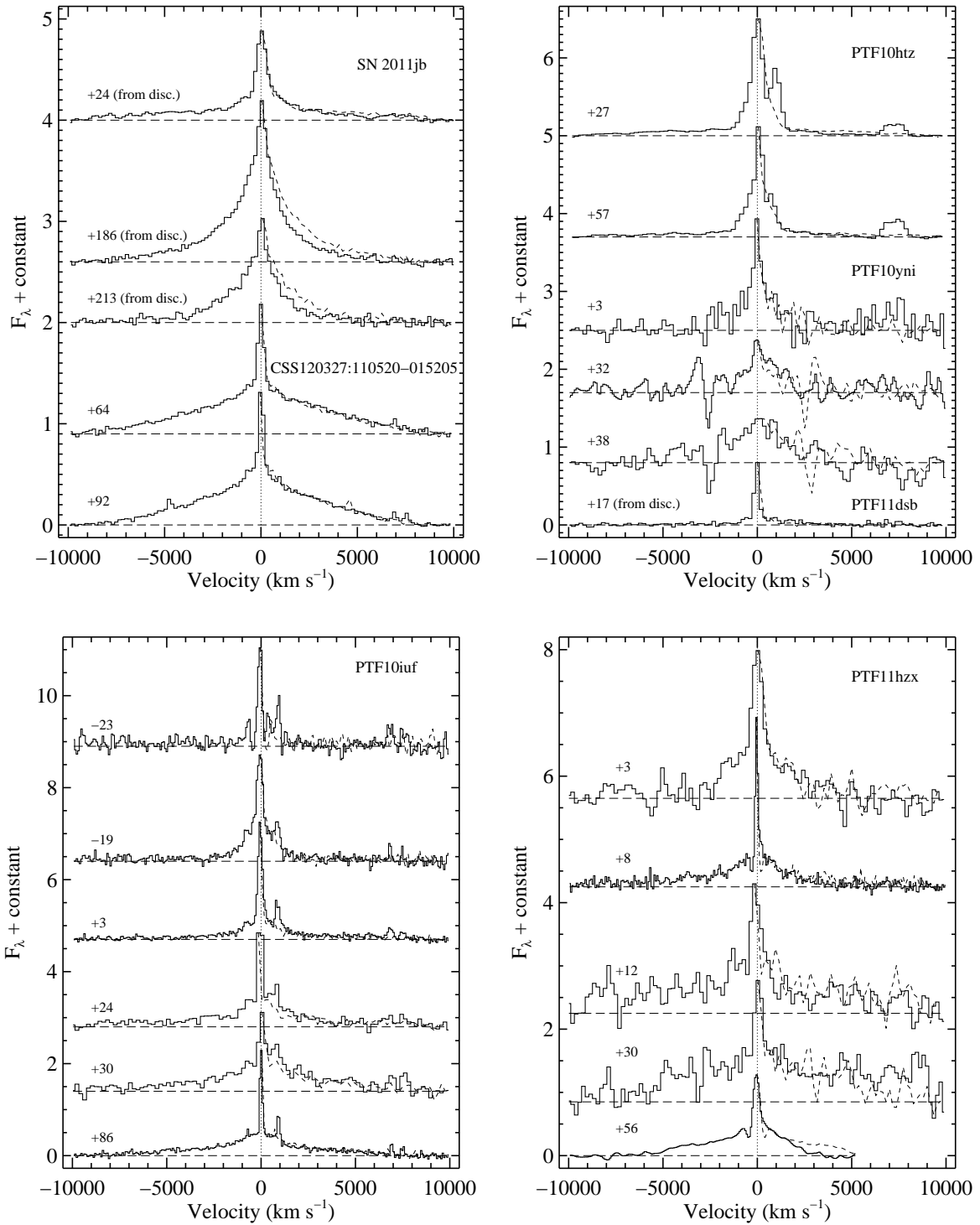


FIG. 15.— The H $\alpha$  profiles of SN 2011jb, CSS120327:110520-015205, PTF10htz, PTF10yni, PTF10iuf, and PTF11hzx. After removing a linear continuum (the long-dashed lines represent the now-horizontal continuum level), we reflect the blue half of the H $\alpha$  profile across the peak flux, yielding the short-dashed lines. The dotted vertical line is the systemic velocity of each object.

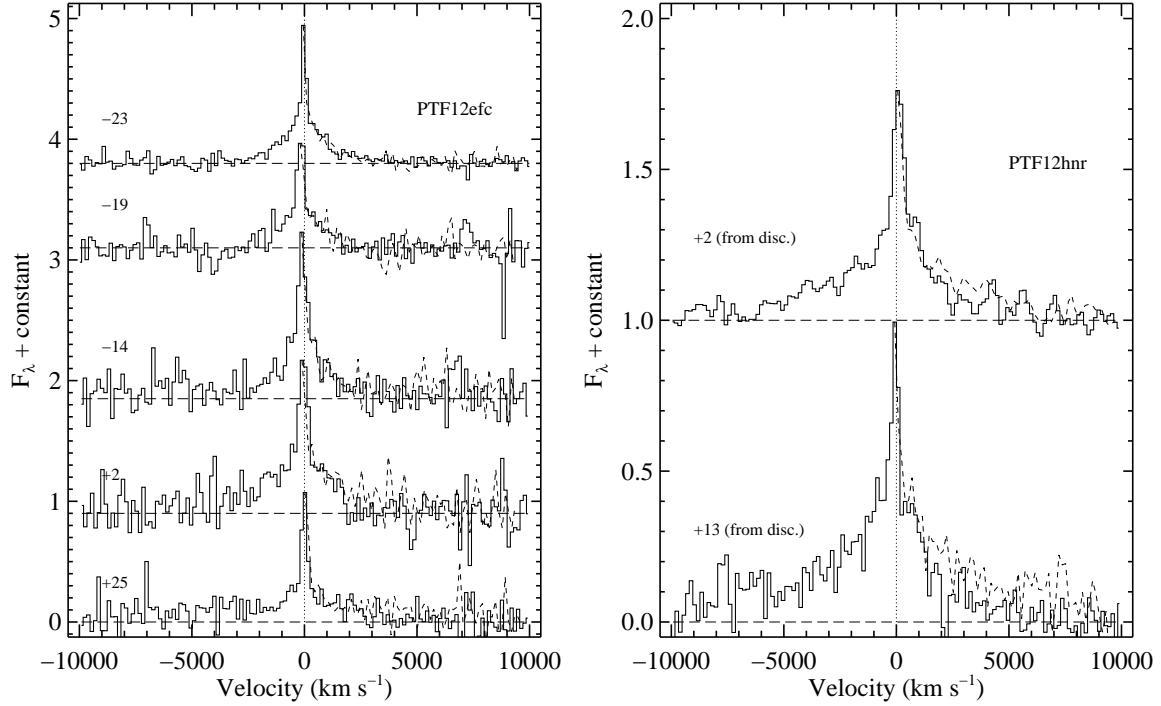


FIG. 16.— The  $H\alpha$  profiles of PTF12efc and PTF12hr. After removing a linear continuum (the long-dashed lines represent the now-horizontal continuum level), we reflect the blue half of the  $H\alpha$  profile across the peak flux, yielding the short-dashed lines. The dotted vertical line is the systemic velocity of each object.

Shen, K. J., Guillochon, J., & Foley, R. J. 2013, *ApJ*, submitted (arXiv:1302.2916)  
 Silverman, J. M., Ganeshalingam, M., Li, W., Filippenko, A. V., Miller, A. A., & Poznanski, D. 2011, *MNRAS*, 410, 585  
 Silverman, J. M. et al. 2012a, *MNRAS*, 425, 1789  
 —. 2012b, *ApJ*, 756, L7  
 Simon, J. D. et al. 2009, *ApJ*, 702, 1157  
 Smith, N., Li, W., Silverman, J. M., Ganeshalingam, M., & Filippenko, A. V. 2011a, *MNRAS*, 415, 773  
 Smith, N., Silverman, J. M., Filippenko, A. V., Cooper, M. C., Matheson, T., Bian, F., Weiner, B. J., & Comerford, J. M. 2012, *AJ*, 143, 17  
 Smith, N. et al. 2011b, *ApJ*, 732, 63  
 Soderberg, A. M. & Frail, D. A. 2005, *The Astronomer's Telegram*, 663, 1  
 Sternberg, A. et al. 2011, *Science*, 333, 856  
 Stritzinger, M., Folatelli, G., & Morrell, N. 2008, *CBET*, 1218, 1  
 Strolger, L. et al. 2002, *AJ*, 124, 2905

Taddia, F. et al. 2012, *A&A*, 545, L7  
 Taubenberger, S. et al. 2011, *MNRAS*, 412, 2735  
 Tremonti, C. A. et al. 2004, *ApJ*, 613, 898  
 Trundle, C., Kotak, R., Vink, J. S., & Meikle, W. P. S. 2008, *A&A*, 483, L47  
 Turatto, M. et al. 2000, *ApJ*, 534, L57  
 Wang, L., Baade, D., Höflich, P., Wheeler, J. C., Kawabata, K., & Nomoto, K. 2004, *ApJ*, 604, L53  
 Webbink, R. F. 1984, *ApJ*, 277, 355  
 Whelan, J. & Iben, Jr., I. 1973, *ApJ*, 186, 1007  
 Wood-Vasey, W. M., Wang, L., & Aldering, G. 2004, *ApJ*, 616, 339  
 Xu, Y., McCray, R., Oliva, E., & Randich, S. 1992, *ApJ*, 386, 181  
 Yamanaka, M. et al. 2009, *ApJ*, 707, L118  
 Yaron, O. & Gal-Yam, A. 2012, *PASP*, 124, 668  
 Zampieri, L., Mucciarelli, P., Pastorello, A., Turatto, M., Cappellaro, E., & Benetti, S. 2005, *MNRAS*, 364, 1419

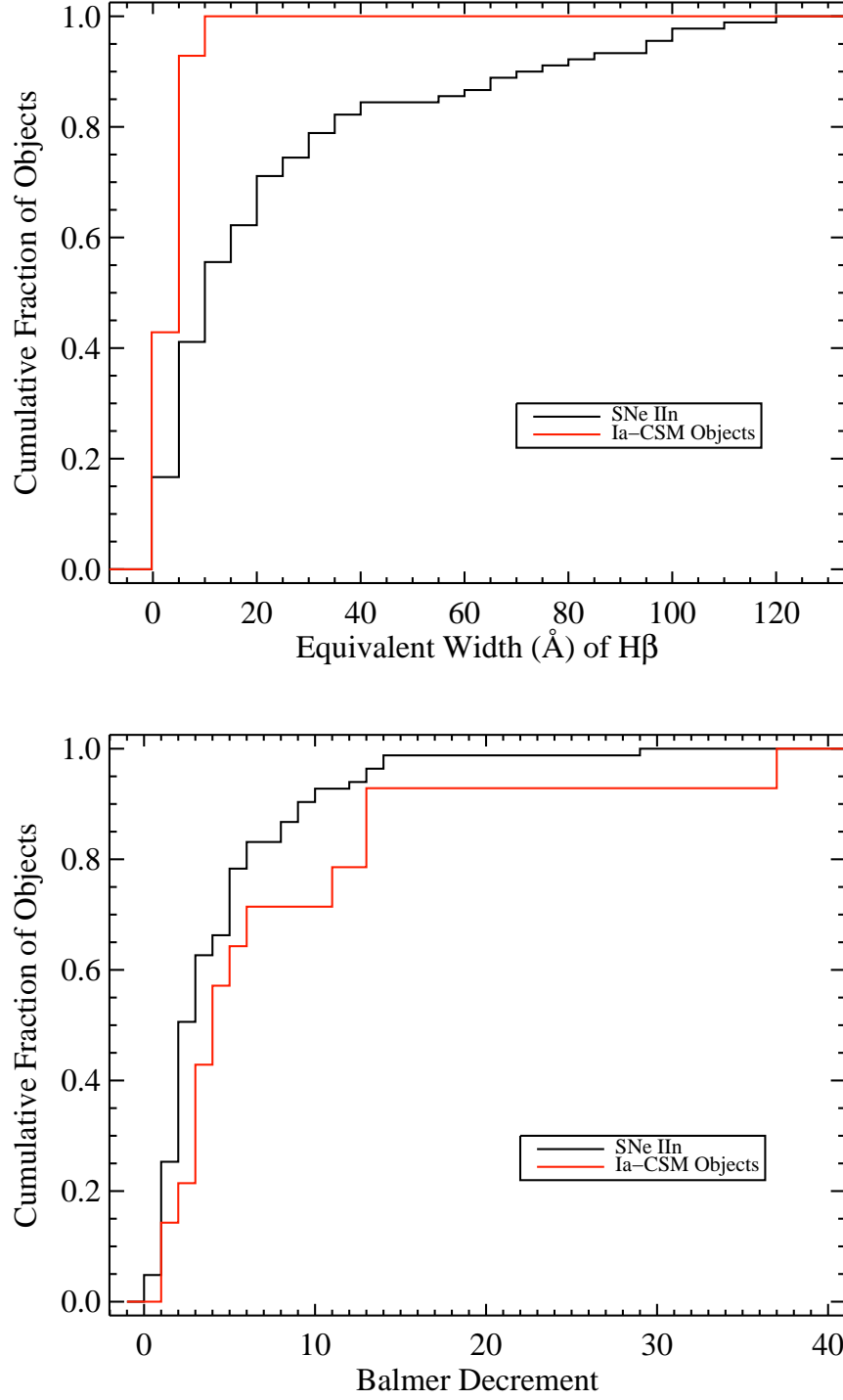


FIG. 17.— Cumulative fraction of H $\beta$  EW (*top*) and H $\alpha$ /H $\beta$  intensity ratio (Balmer decrement; *bottom*) for all SNe IIIn from the Berkeley SN Group’s database and PTF (black), and for SNe Ia-CSM with spectra presented herein (red). The median values were used when there were multiple measurements for a given object.

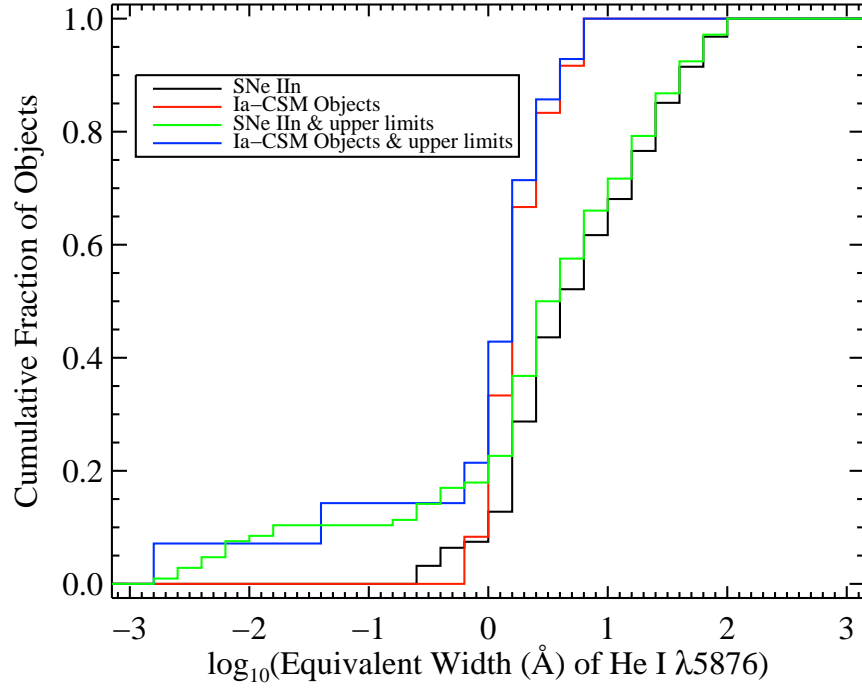


FIG. 18.— Cumulative fraction of He I  $\lambda 5876$  EW for all SNe IIa from the Berkeley SN Group’s database and PTF (black), and for SNe Ia-CSM with spectra presented herein (red). Also shown are the He I  $\lambda 5876$  EWs for SNe Ia-CSM including upper limits (blue) and for SNe IIa as well (green). The median EW value is used when there are multiple measurements for a given object.